THE UNIVERSITY OF MICHIGAN RESEARCH INSTITUTE
ANN ARBOR, MICHIGAN

THEORY OF THE CRESTATRON: A FORWARD-WAVE AMPLIFIER

TECHNICAL REPORT NO. 27

Electron Tube Laboratory
Department of Electrical Engineering

By

Joseph E. Rowe

Project 2750

CONTRACT NO. AF30(602)-1845
DEPARTMENT OF THE AIR FORCE
PROJECT NO. 4506, TASK NO. 45152
PLACED BY: THE ROME AIR DEVELOPMENT CENTER
GRIFFISS AIR FORCE BASE, NEW YORK

September, 1958

TABLE OF CONTENTS

ABSTRACT

A new type of forward-wave traveling-wave amplifier has been developed which offers moderate gain (10 to 20 db) and high operating efficiency coupled with a very short length (4 to 6 wavelengths), thus reducing the size of focusing magnet required. The operation of the device depends upon the beating effect produced when the three forward waves described in the traveling-wave tube theory travel along the slow-wave structure. The device, named the Crestatron, operates with voltages sufficiently high so that there are no growing waves and the gain is determined by the beam injection velocity and not by the length of the tube. The operation of the Crestatron has been analyzed with both a large-C linear theory and a large-signal theory of traveling-wave tubes. The effect of circuit loss on gain is to reduce the beating gain at a rate of 12 db per unit d from the d = 0 gain. Large-signal calculations indicate that high saturation efficiency characterizes this mode of operation.

LIST OF ILLUSTRATIONS

LIST OF ILLUSTRATIONS

(Continued)

THEORY OF THE CRESTATRON: A FORWARD-WAVE AMPLIFIER*

INTRODUCTION

It is well known that the operation of backward-wave devices, both O-type and M-type, depends on an interference phenomenon resulting from the beating between waves propagating along an r-f structure. It can also be shown that in forward-wave devices such as the traveling-wave amplifier gain can occur due to the beating of waves traveling on the r-f structure, providing that the length is correct. The magnitude of this gain for any given set of circuit and operating parameters is determined by the relative injection velocity b rather than by the length of the tube as in the case of the conventional traveling-wave amplifier.

A voltage gain is produced in the Crestatron by a beating between the three forward waves propagating on the slow-wave structure. The device is operated with a beam velocity such that $b > b_{x_1=o}$ and hence there are no growing waves. The gain is achieved by adjusting the tube length to the proper value such that all the waves, one of which is out of phase with the others at the input, add together to give an r-f voltage greater than that at the input. Hence there is not voltage gain in the sense of that produced by growing waves but there is gain if the tube is considered to be a two-port network. The amount of gain is determined by the value of b and decreases as the beam velocity is raised above that at which growing waves cease to exist. The gain characteristics of the

---

*Presented at the Sixteenth Conference on Electron Tube Research, Quebec, Canada; June 25-27, 1958.

Crestatron can be calculated from the small-signal theory and these calculations also give information on the CN bandwidth achievable in the device.

The large-signal theory of traveling-wave amplifiers[1] has been used to calculate the nonlinear performance of the Crestatron in terms of the gain achievable and the expected operating efficiency.

Ample experimental evidence[2] has already been offered to verify the theory and indicate that high efficiency is obtained with short length and moderate gains. During the course of this work it was learned that Mourier and Sugai have shown that a similar type of operation is possible with the forward-wave magnetron amplifier.[3] They treated the special case of small C, no space charge and zero circuit loss. These conditions in the magnetron amplifier give rise to two forward traveling waves which under certain conditions can beat with one another to produce gain.

DERIVATION OF THE GAIN EQUATION

The three forward waves propagating on a traveling-wave tube r-f structure are known to vary in the following manner:[4]

$$e^{-\Gamma z} = e^{-j\beta z} \cdot e^{\beta C \delta z} \quad , \tag{1}$$

where β is the wave phase constant and is equal to β_e at synchronism. The normalized voltage V_z/V at any point along the r-f structure may be written in terms of the amplitudes of the three waves, neglecting space charge, as

$$\frac{V_z}{V} = e^{-j\frac{\theta}{C}} \left[\frac{V_1}{V} e^{\delta_1 \theta} + \frac{V_2}{V} e^{\delta_2 \theta} + \frac{V_3}{V} e^{\delta_3 \theta} \right] \tag{2}$$

---

1. Rowe, J. E., "A Large-Signal Analysis of the Traveling-Wave Amplifier: Theory and General Results", Trans. PGED-IRE, ED-3, No. 1, 39-56, January, 1956.
2. Caldwell, J. J., and Hoch, O. L., "Large-Signal Behavior of High Power Traveling-Wave Amplifiers", Trans. PGED-IRE, ED-3, 6-18, January, 1956.
3. Mourier, G., and Sugai, I., private communication.
4. Pierce, J. R., Traveling-Wave Tubes, D. Van Nostrand Co., New York; 1950.

where $\delta_i = x_i + jy_i$, $i = 1,2,3$;

V_i/V = normalized voltage amplitude of each wave;

$\theta \triangleq \beta Cz = 2\pi CN$;

N = structure length in wavelengths; and

C = gain parameter.

From the small-signal theory of the traveling-wave tube, the following expressions for the r-f convection current and velocity are obtained by retaining terms proportional to C:

$$\frac{(1+jC\delta_1)}{\delta_1} V_1 + \frac{(1+jC\delta_2)}{\delta_2} V_2 + \frac{(1+jC\delta_3)}{\delta_3} V_3 = \left(\frac{ju_oC}{\eta}\right) \tilde{v} \qquad (3)$$

and

$$\frac{(1+jC\delta_1)}{\delta_1^2} V_1 + \frac{(1+jC\delta_2)}{\delta_2^2} V_2 + \frac{(1+jC\delta_3)}{\delta_3^2} V_3 = \left(\frac{-2V_oC^2}{I_o}\right) \tilde{i} \ , \qquad (4)$$

where η = e/m, charge-to-mass ratio of the electron,

$\tilde{v}$ = r-f velocity in the stream,

$\tilde{i}$ = r-f convection current in the stream,

V_o = d-c stream voltage, and

I_o = d-c stream current.

If an unmodulated stream is injected at z = 0 and an r-f signal level V is applied to the r-f structure at that point, the boundary conditions require that the right-hand sides of Eqs. 3 and 4 be zero and that

$$V = V_1 + V_2 + V_3 \ . \qquad (5)$$

Equations 3, 4, and 5 may be solved simultaneously to give the normalized amplitudes of the individual waves. The general result is shown below.

$$\frac{V_i}{V} = \left[1 + \frac{1+jC\delta_i}{1+jC\delta_{i+1}} \left(\frac{\delta_{i+1}}{\delta_i}\right)^2 \frac{\delta_{i+1}-\delta_i}{\delta_{i+1}-\delta_{i+2}} + \frac{1+jC\delta_i}{1+jC\delta_{i+2}} \left(\frac{\delta_{i+2}}{\delta_i}\right)^2 \frac{\delta_i-\delta_{i+1}}{\delta_{i+1}-\delta_{i+2}}\right]^{-1} \qquad (6)$$

where $\delta_i \equiv \delta_{i+3}$. Equation 6 gives the total voltage associated with each wave and in the absence of space charge also gives the circuit voltage. The effect of passive modes or space charge is to reduce the circuit voltage from the value predicted by Eq. 6. The ratio of the circuit voltage to the total voltage is found from the ratio of the second term on the right-hand side of the following familiar quartic determinantal equation to the total right-hand side[5] of Eq. 6:

$$\delta^2 = \frac{(1+jC\delta)^2\,[1+C(b-jd)]}{\left[-b+jd+j\delta+C\left(jbd - \frac{b^2}{2} + \frac{d^2}{2} + \frac{\delta^2}{2}\right)\right]} -4QC\,(1+jC\delta)^2 \quad . \tag{7}$$

The general result for the circuit component of voltage is

$$\frac{V_{ci}}{V_i} = 1 + 4QC\,\frac{(1+jC\delta_i)^2}{\delta_i^2} \quad . \tag{8}$$

Equations 6 and 8 have been obtained by Brewer and Birdsall.[6]

Thus the voltage along the r-f structure may be written in general, including the effects of finite C and space charge QC, as

$$\frac{V_z}{V} = e^{-j\frac{\theta}{C}} \sum_{i=1}^{3} \left(\frac{V_i}{V}\right)\left(\frac{V_{ci}}{V_i}\right) e^{\delta_i\theta} \quad , \tag{9}$$

where $\delta_i \equiv \delta_{i+3}$. When C is small and the effect of passive modes or space charge is negligible, Eqs. 6 and 8 reduce to the following familiar form.

$$\frac{V_i}{V} = \frac{\delta_i^2}{(\delta_i - \delta_{i+1})\,.(\delta_i - \delta_{i+2})} \tag{10}$$

---

5. Ibid., p. 113, Eq. 7.13 with corrections.
6. Brewer, G. R., and Birdsall, C. K., "Normalized Propagation Constants for a Traveling-Wave Tube for Finite Values of C," Tech. Memo. No. 331, Hughes Research and Development Laboratories, Culver City, California; October 1953.

and

$$\frac{V_{ci}}{V_i} = 1 \quad . \tag{11}$$

The voltage gain is written as

$$G_{db} = 10 \log \left(\frac{V_z V_z^*}{V V^*} \right) = 10 \log \left| \left(\frac{V_z}{V} \right)^2 \right| \quad . \tag{12}$$

It is important to note that, unlike conventional standing waves on a transmission line, each wave sees the r-f structure characteristic impedance at all points along the line.

The gain that occurs when the velocity parameter b is greater than that for which the growth constant of the growing wave is zero is, as mentioned before, due to a beating effect between the three small-signal waves which are set up at the input and propagate along the r-f structure. The interaction is primarily between the circuit wave and the slow space-charge wave. It will be seen later that the fast space-charge wave is excited to a negligible extent. This is the same basic mode of operation as in the backward-wave device of both the traveling-wave tube and crossed-field types. As the three waves travel along the structure the phase relationship between the r-f current in the beam and the r-f field on the circuit changes and at certain points along the circuit the phase is such that energy is transferred to the circuit. At the same time there are certain regions along the tube where the phase relationship between the beam current and the circuit field is such that energy is fed from the circuit back to the beam. The gain in this mode of operation depends upon the relative injection velocity b for any given set of tube parameters rather than on the length as in the case of the conventional traveling-wave tube.

The Crestatron is inherently more efficient than the backward-wave devices which operate on the same principle because the modulation in the stream

and the field on the circuit producing the modulation travel in the same direction, whereas in the backward-wave device the modulation in the beam and the circuit field travel in opposite directions. In the backward-wave device the circuit field is strongest where the modulation is weakest and vice versa.

Mathematically speaking all the energy is abstracted from the beam at the input since in satisfying the boundary conditions energy is put into setting up the three circuit waves. Then the circuit length is simply adjusted so that at the end of the tube the wave energies all add in phase. It should be recalled that in this region of operation the propagation constants are purely imaginary, giving rise to real voltage amplitudes, and at the input one voltage component is 180 degrees out of phase with the other two.

SMALL-SIGNAL GAIN

It was pointed out above that the normalized voltage amplitudes are purely real since the propagation constants are purely imaginary when $b > b_{x_1=0}$. For fixed values of C, QC, and d the gain may be calculated from Eqs. 6 and 21 as a function of θ for particular values of b. Typical gain curves are shown in Figs. 1 and 2. The above gain equations are valid for all values of b and it is seen from the figures that the normal exponential gain is obtained when $x_1 \neq 0$. The gain curves were plotted over a range of 6π radians to indicate their repetitive nature. The effect of circuit loss on the gain vs. length is shown in Figs. 3 and 4, and it is seen that the presence of loss reduces the gain particularly for large values of θ. However, for small values of d the gain at the first maximum is not appreciably reduced.

The results plotted in Fig. 3 do not show the large negative dip in the gain curve for b = 0 that Brewer and Birdsall[7] found. The fact that they

---

7. Brewer, G. R., and Birdsall, C. K., "Traveling-Wave Tube Propagation Constants", Trans. PGED-IRE, ED-4, No. 2, pp. 140-144; April, 1957 (Figure 2).

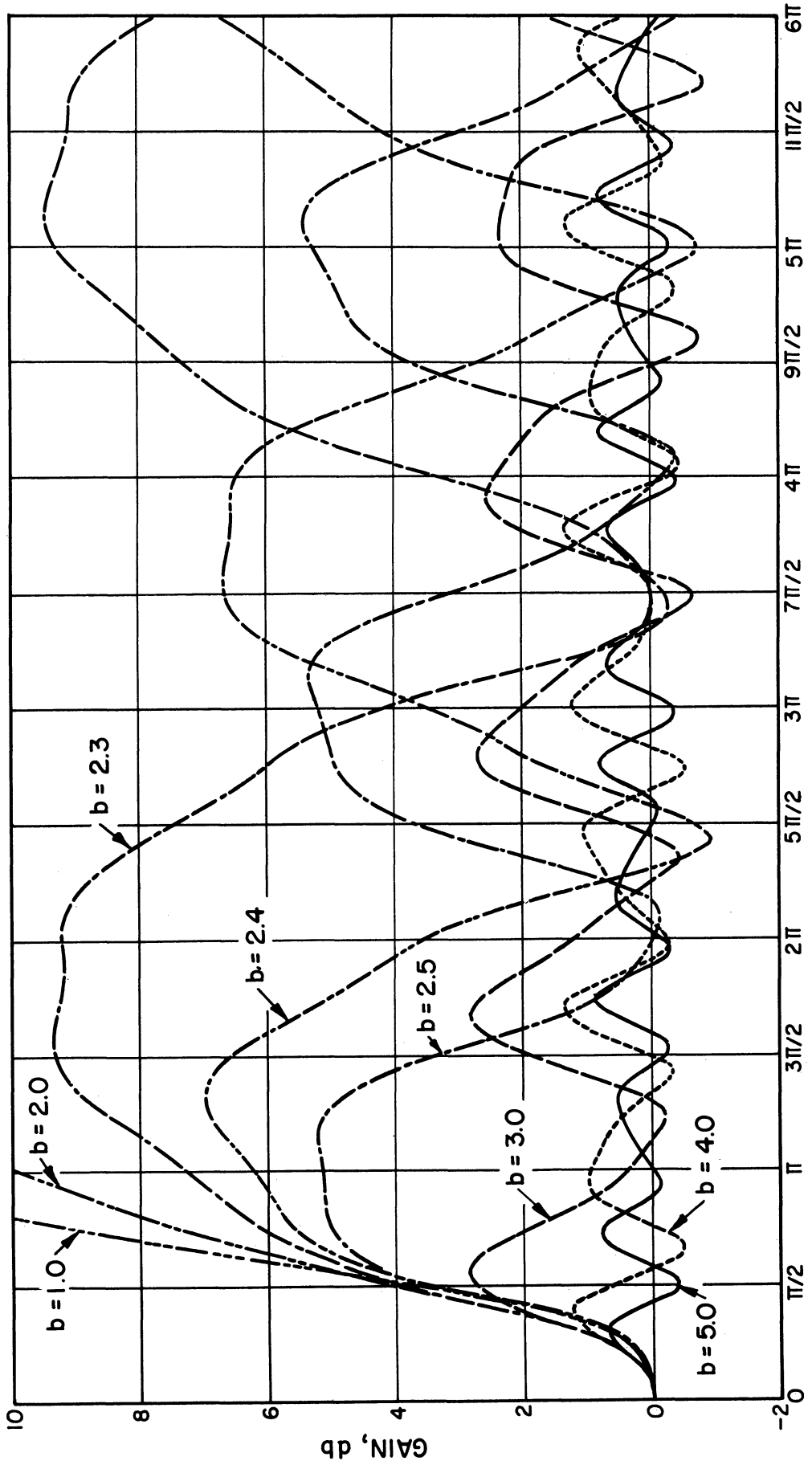

FIG. 1 GAIN VS. LENGTH. (C = 0.05, QC = 0.125, d = 0, $b_{x_1=0} = 2.20$)

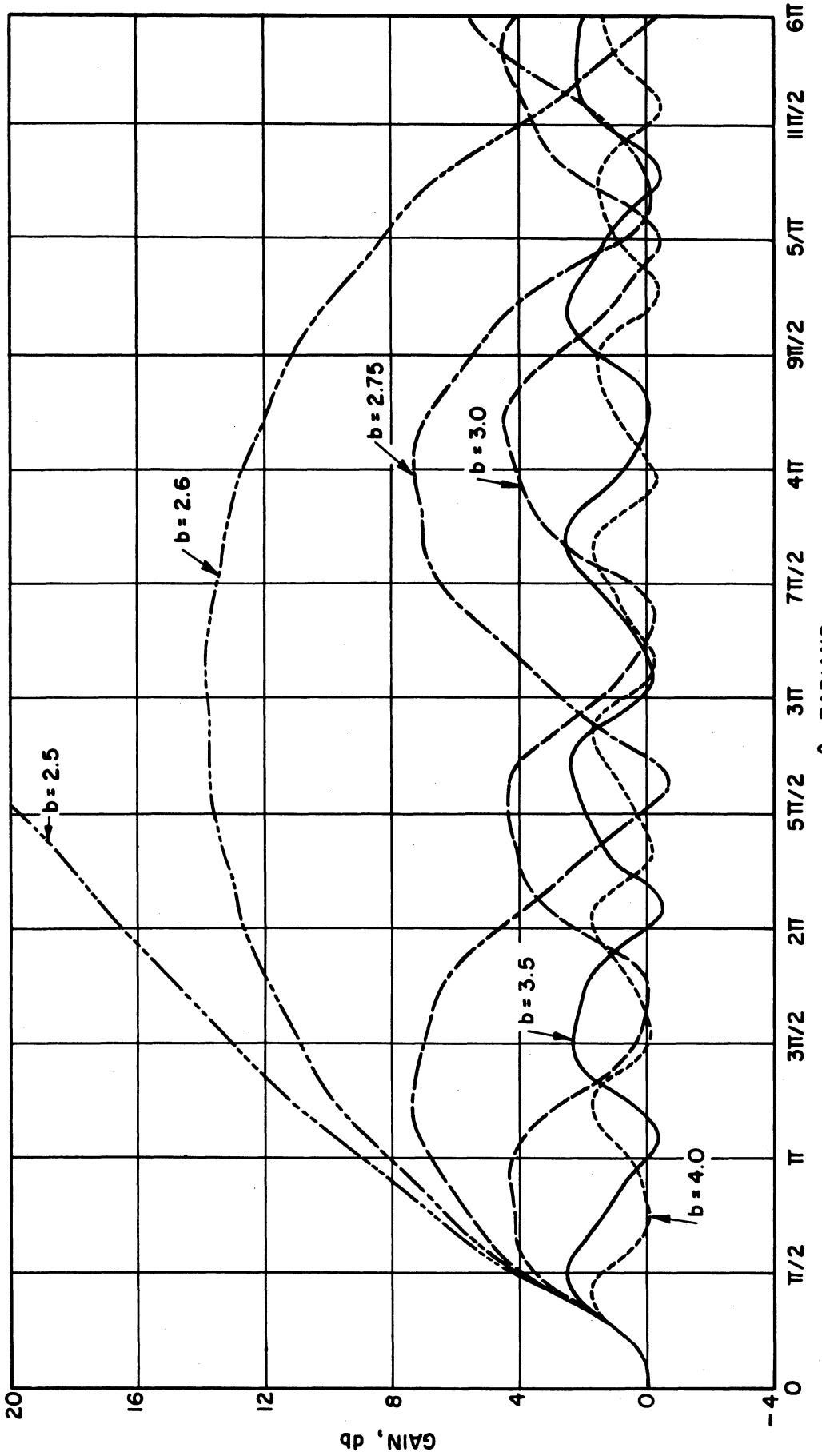

FIG. 2 GAIN VS. LENGTH. ($C = 0.1$, $QC = 0.25$, $d = 0$, $b_{x_1=0} = 2.57$)

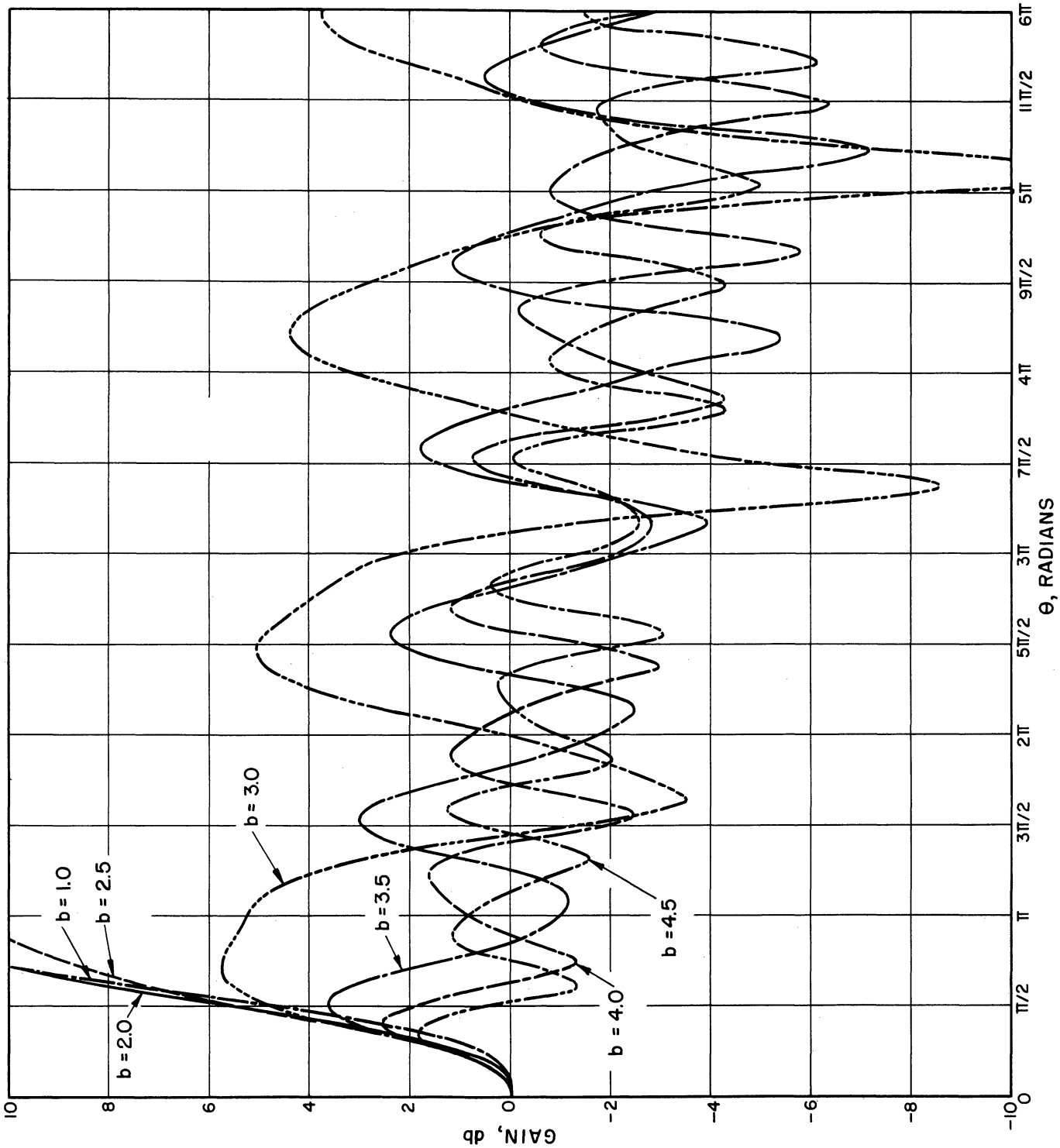

FIG. 3 GAIN VS. LENGTH. ($C = 0.2$, $QC = 0.125$, $d = 0.025$, $b_{x_1=0} > 3.0$)

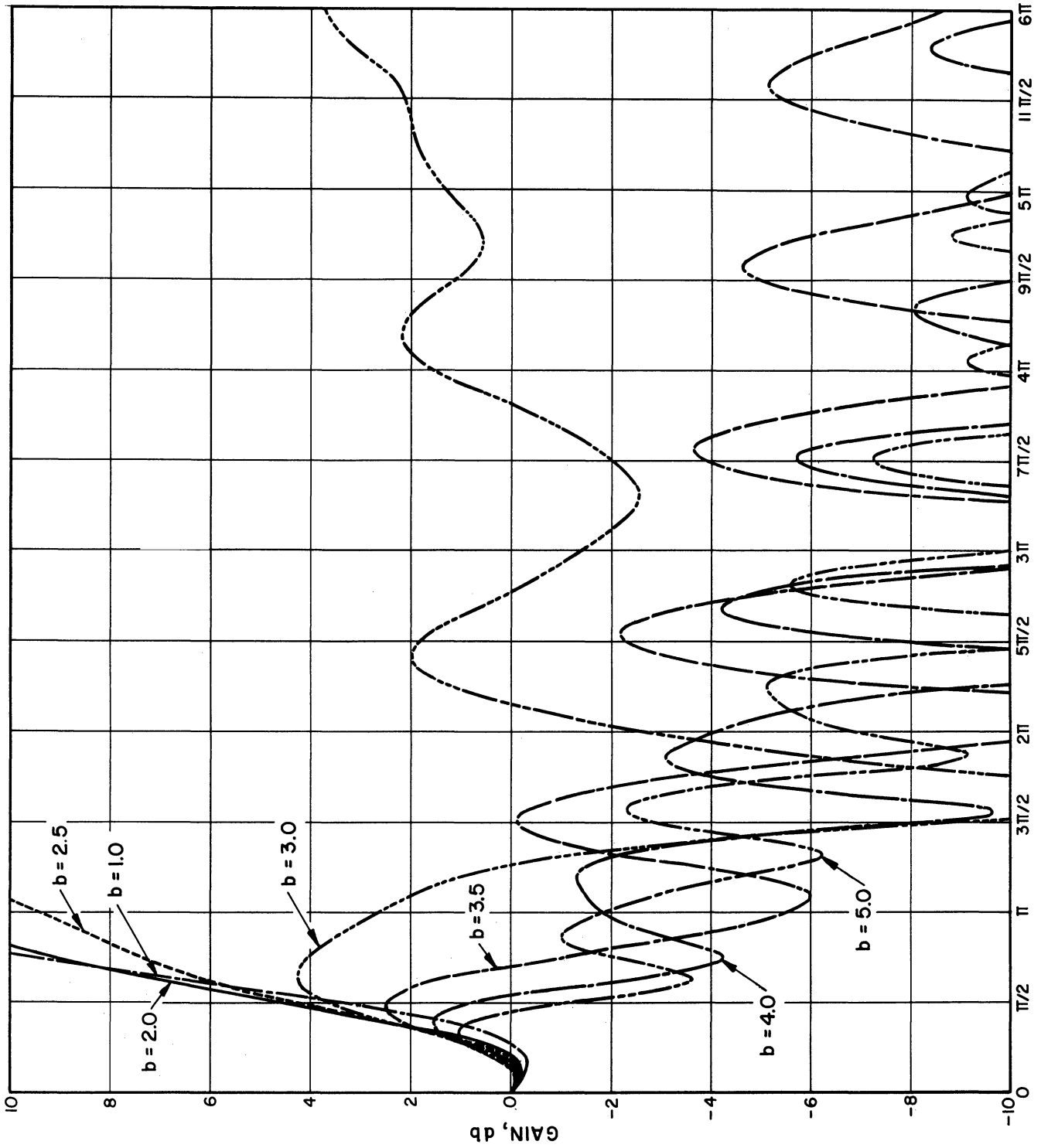

FIG. 4 GAIN VS. LENGTH. (C = 0.2, QC = 0.125, d = 0.125, $b_{x,=o} > 3.0$)

assumed a QC = 0.25 whereas the above data are for QC = 0.125 is of little consequence to this discrepancy. It is believed that these results of Brewer and Birdsall are incorrect since to compute gain they used the small-C equations, which are not valid when C = 0.2 and QC = 0.25. It should be pointed out that only very small dips in the gain curves were noted in the large-signal calculations, as is predicted here. Large negative dips in the gain seem to occur at b = -1 for most values of C and QC and for positive values of b when d is large.

The gain curves of Fig. 5 show that gain is also achieved for negative values of b such that $x_1 = 0$. Negative values of b correspond to operating voltages less than the synchronous voltage; and the resulting gains are less than those obtained with large values of b.

When the loss parameter is zero all maxima of the gain curve are approximately equal (the slight variations and lack of periodicity will be explained later), but when $d \neq 0$ the first maximum will be highest and subsequent peaks will generally be lower. This merely emphasizes the fact that when circuit loss is significant the Crestatron length should be chosen so as to operate on the first maximum of the gain curve.

It is seen from the gain curves that for fixed b and variable θ the curves are nonperiodic within the interval 6π and exhibit periodic undulations in amplitude. The explanation of this phenomenon is contained in Eq. 9 for the voltage amplitude vs. distance. The lack of periodicity with 2π and the undulating peak amplitudes are a result of the product of $\exp(-j\,\theta/C)$ and $\exp(\delta_i\theta)$, where each represents a vector rotating about the origin as a function of θ. The rate of rotation of the first vector is related to 1/C, which is typically between 5 and 20, and the rate of rotation of the second is determined by δ_i, which varies between 1 and 3. The first, then, perturbs the second as a modulation and the fact that δ_i is nonintegral in general means that it is not

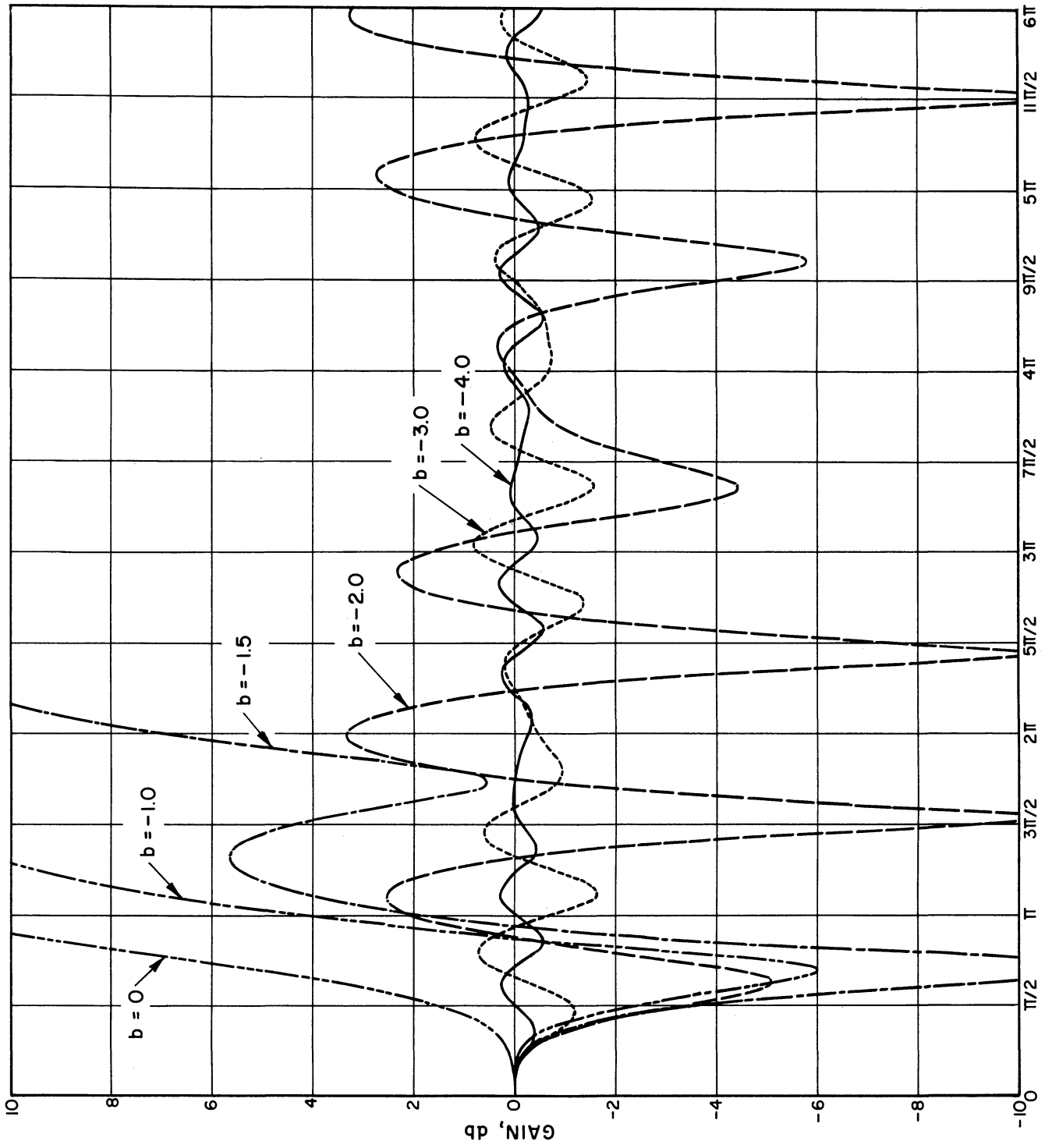

FIG. 5 GAIN VS. LENGTH. ($C = 0.10$, $QC = 0.125$, $d = 0$, $b_{x_1=0} = 2.34$)

periodic with 2π. It may be that θ must travel through $2m\pi$ radians with m very large before a periodicity is apparent, if ever.

The above phenomenon indicates that there is something more than a simple beating effect occurring between the waves. In fact there is a continual slipping of one wave with respect to the others along the tube. This process accounts for the fact that there is or may be a net interchange of energy between the beam and the circuit in a device of infinite length. It is interesting to examine the condition necessary for the gain curve to be periodic with period $2m\pi$ and also the condition required for the peak amplitudes to be constant. In fact these two conditions would result in a gain curve that is exactly reproduced every 2π radians.

In Eq. 9 for V_z/V, when b is held fixed, the phase condition is determined by the product

$$e^{-j\frac{\theta}{C}} \cdot e^{\delta_i \theta} = e^{j\theta\left(y_i - \frac{1}{C}\right)} , \tag{13}$$

since $x_i = 0$. Thus in order for the phase to be periodic with $2m\pi$

$$n\left(y_i - \frac{1}{C}\right) = 2m\pi \quad . \tag{14}$$

Solving for y_i gives

$$y_i = \frac{2m\pi}{n} + \frac{1}{C} , \tag{15}$$

where n and m are independent integers. Thus for phase periodicity the value of y_i must be equal to a constant plus some integral or subintegral multiple of 2π. When $C \rightarrow 0$, $y_i = 1/C$ and all the waves travel at approximately the same rate, thus maintaining the same relative phase positions with respect to one another. This results in a constant-amplitude vector rotating about the origin with a period of 2π radians. Thus the gain curve will be periodic in amplitude also.

Under very restricted conditions a simplified expression for the gain of the Crestatron may be obtained from Eq. 9. When $C \to 0$, $QC = 0$, $d = 0$, and b is sufficiently large that the propagation constants are purely imaginary, it can be determined that the δ_i's are given approximately by

$$\delta_1 \approx -j/b^{1/2} ,$$

$$\delta_2 \approx -jb,$$

and

$$\delta_3 \approx j/b^{1/2} . \tag{16}$$

Substitution of Eq. 16 into Eq. 9 yields for the gain, after some simplification,

$$\left|\frac{V_z}{V}\right|^2 = \left(\frac{1}{1-b^3}\right)^2 \left[1 + b^6 + (b^3-1)\sin^2\frac{\theta}{b^{1/2}} - 2b^3\left\{\cos\theta b \cos\frac{\theta}{b^{1/2}} + b^{3/2}\sin\theta b \sin\frac{\theta}{b^{1/2}}\right\}\right] . \tag{17}$$

Since b is usually greater than 2.5, Eq. 17 can be further simplified to

$$\left|\frac{V_z}{V}\right|^2 = 1 + \frac{1}{b^3}\left[\sin^2\frac{\theta}{b^{1/2}} - 2\cos\theta b \cos\frac{\theta}{b^{1/2}} + b^{3/2}\sin\theta b \sin\frac{\theta}{b^{1/2}}\right] . \tag{18}$$

A useful expression for predicting the value of CN at the first maximum of the gain curve may be obtained by differentiating Eq. 17 with respect to θ and setting the result equal to zero. In this way

$$\sin\frac{\theta}{b^{1/2}}\left[\cos\frac{\theta}{b^{1/2}} - b^3\cos\theta b\right] = 0 . \tag{19}$$

Thus maxima and minima in the gain occur for

$$\sin\frac{\theta}{b^{1/2}} = 0$$

or

$$CN = \frac{n\, b^{1/2}}{2} \qquad n = 0,1,2,... \tag{20}$$

The other condition is

$$\cos \Theta b = \frac{\cos \frac{\Theta}{b^{1/2}}}{b^3} \approx 0 \quad \text{for large } b$$

or

$$CN = \frac{2n+1}{4b}, \qquad n = 0,1,2,... \tag{21}$$

Equation 21 predicts quite accurately the distance to the first maximum in the gain curve when n = 1. Thus

$$\text{CN to first maximum} = \frac{0.75}{b} . \tag{22}$$

Equations 20 and 21 coupled with information on the second derivative of the gain curve may be used to determine subsequent maxima in the gain vs. Θ curve.

In addition to gain vs. length curves for fixed b, a set of gain curves may be obtained for fixed tube length with variable voltage or b. Typical curves of this type are shown in Figs. 6 and 7. The main hump in the gain curve vs. b is of course due to exponential gain and the other lower peaks correspond to gain through beating waves. When $C \rightarrow 0$, $QC = 0$, and $d = 0$ the gain vs. b curve will be symmetrical with respect to b since maximum exponential gain occurs at synchronism.

MAGNETIC FIELD REQUIREMENT

The limiting stream perveance which can be transmitted through a cylindrical drift tube or helix due to space-charge spreading is given by[8]

$$\text{Perveance} = 38.6 \times 10^{-6} \left(\frac{d}{\ell}\right)^2 , \tag{23}$$

where d = helix diameter, and

ℓ = helix length.

8. Pierce, J. R., Theory and Design of Electron Beams, D. Van Nostrand Co., New York; 1954, p. 151.

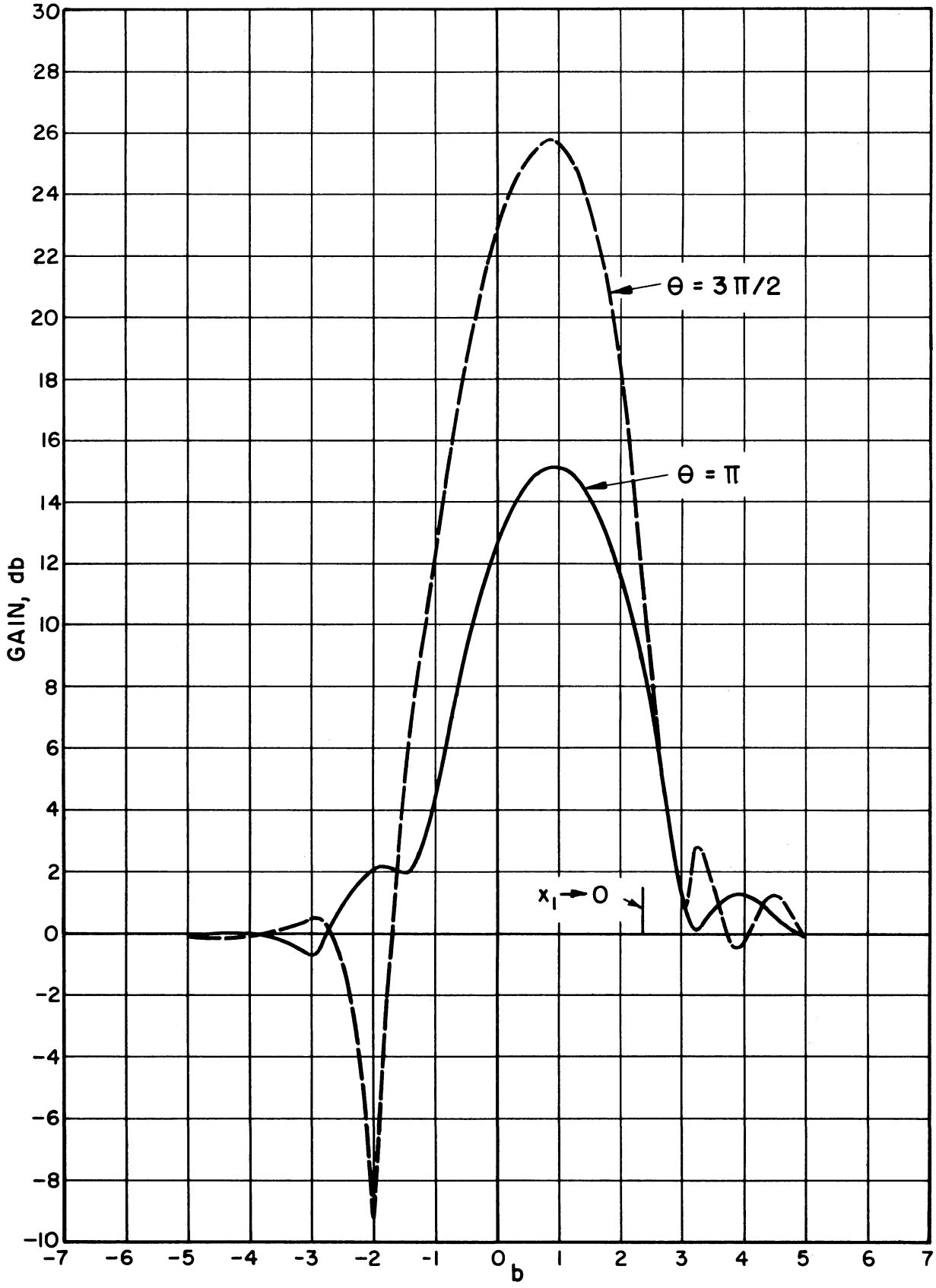

FIG. 6 GAIN VS. INJECTION VELOCITY FOR FIXED TUBE LENGTH. (C = 0.1, QC = 0.125, d = 0)

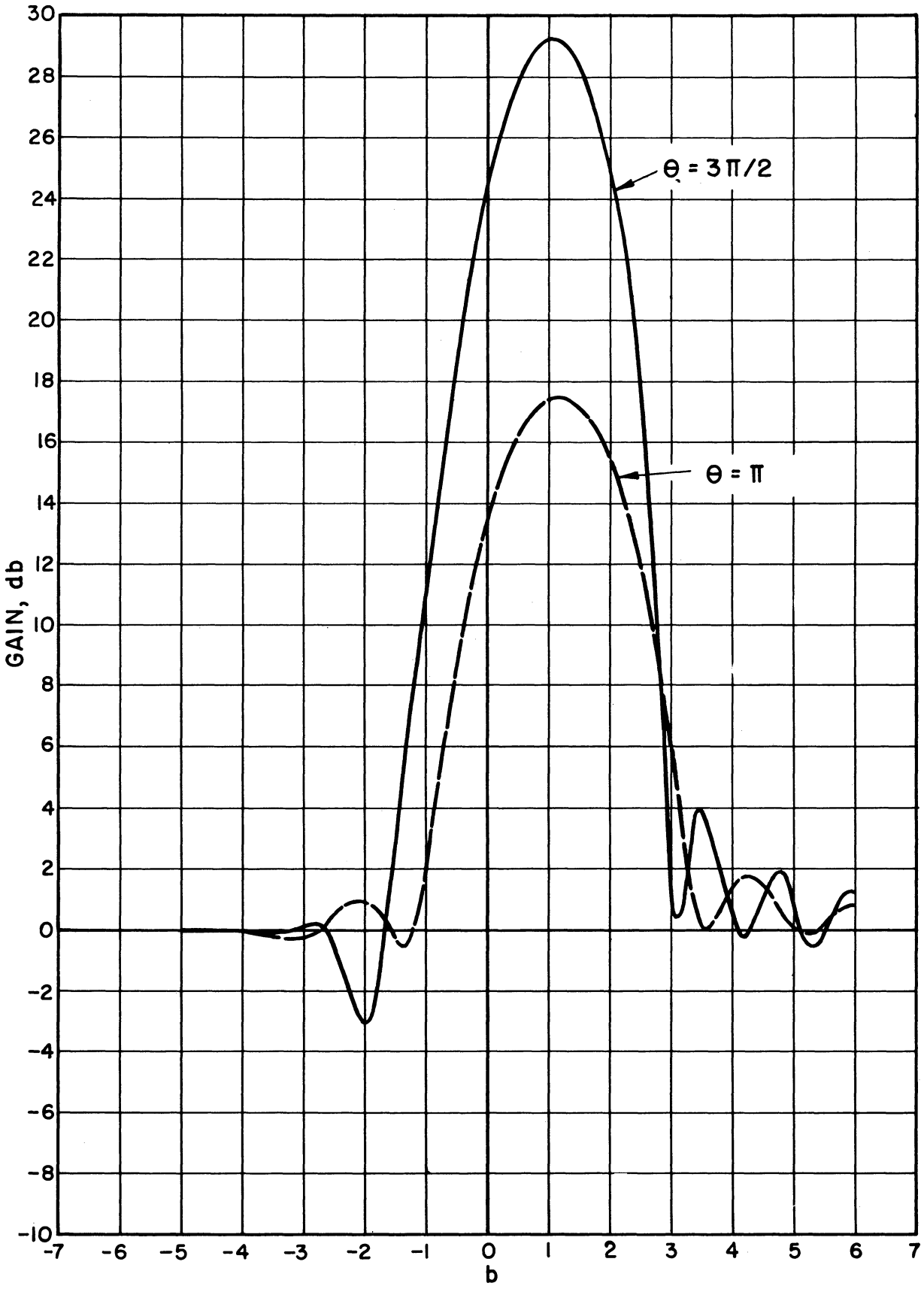

FIG. 7 GAIN VS. INJECTION VELOCITY FOR FIXED TUBE LENGTH. (C = 0.2, QC = 0.125, d = 0)

The following familiar relations for traveling-wave tubes are recalled

$$CN_s = \left(\frac{FK_s I_o}{4V_o}\right)^{1/3} \frac{\ell f}{u_o} \quad , \tag{24a}$$

$$u_o = (2\eta V_o)^{1/2} = \lambda_s f \quad , \tag{24b}$$

$$\frac{u_o}{v_o} = 1 + Cb \quad , \tag{24c}$$

and

$$\gamma a = 2\pi a/\lambda_g \quad . \tag{24d}$$

The helix impedance FK_s used in Eq. 24a may be written as

$$FK_s = \frac{506\ FK_s'\ (1+Cb)}{V_o^{1/2}} \quad , \tag{25}$$

where F = the impedance reduction factor due to dielectric loading and space harmonics and

K_s' = sheath-helix impedance as given in Fig. A6.5 in Pierce.[9]

Combining Eqs. 23 through 25 yields

$$CN_s = 0.054 \frac{(FK_s')^{1/3}}{(1+Cb)^{2/3}} (\gamma a) \left(\frac{\ell}{d}\right)^{1/3} \quad . \tag{26}$$

From Eq. 26 can be calculated the maximum length of structure which can be used when no magnetic focusing field is present and the stream is allowed to spread under the influence of space-charge forces. Of course, the stream must be injected in a convergent manner aimed toward the center of the structure and then it is allowed to expand, resulting in a divergent stream at the output end. Allowance will also have to be made for stream spreading due to the presence of r-f fields on the structure. The following typical values of the parameters in Eq. 26 are used to evaluate CN_s:

---

9. Pierce, J. R., Traveling-Wave Tubes, D. Van Nostrand Co., New York; 1950.

$$\gamma a = 1.5$$

$$(FK_s')^{1/3} = 2.2$$

$$(1+Cb)^{2/3} = 1.3$$

$$\left(\frac{\ell}{d}\right)^{1/3} = 2.5 \quad .$$

Using the above values gives

$$CN_s = 0.34 \quad .$$

This value of CN_s is compatible with the lengths required for Crestatron operation. Hence under some conditions it may be possible to operate the Crestatron with little or no magnetic focusing field. Electrostatic focusing systems are sometimes possible depending upon the structure type.

BANDWIDTH

The bandwidth of the Crestatron may be determined from the gain curves shown in Figs. 1 through 4. The CN bandwidth can be as large as ± 50 percent between 3-db points on the gain curve. If the impedance of the structure remained constant over this range then the Crestatron would have a frequency bandwidth of 3:1. In general impedance variations will limit this figure to some lower value.

MAXIMUM GAIN VS. C AND QC

It was pointed out earlier that the voltages are purely real in the Crestatron and at the input one voltage is 180 degrees out of phase with the other two. Thus the maximum gain will occur when the three waves all add in phase. The value of b for which $x_1 = 0$ has been computed from the quartic determinantal equation and is shown in Fig. 8 for a range of values of C and QC with zero loss. When $d \neq 0$ x_1 is not exactly zero anywhere but does drop to less than one percent of its maximum value for large b.

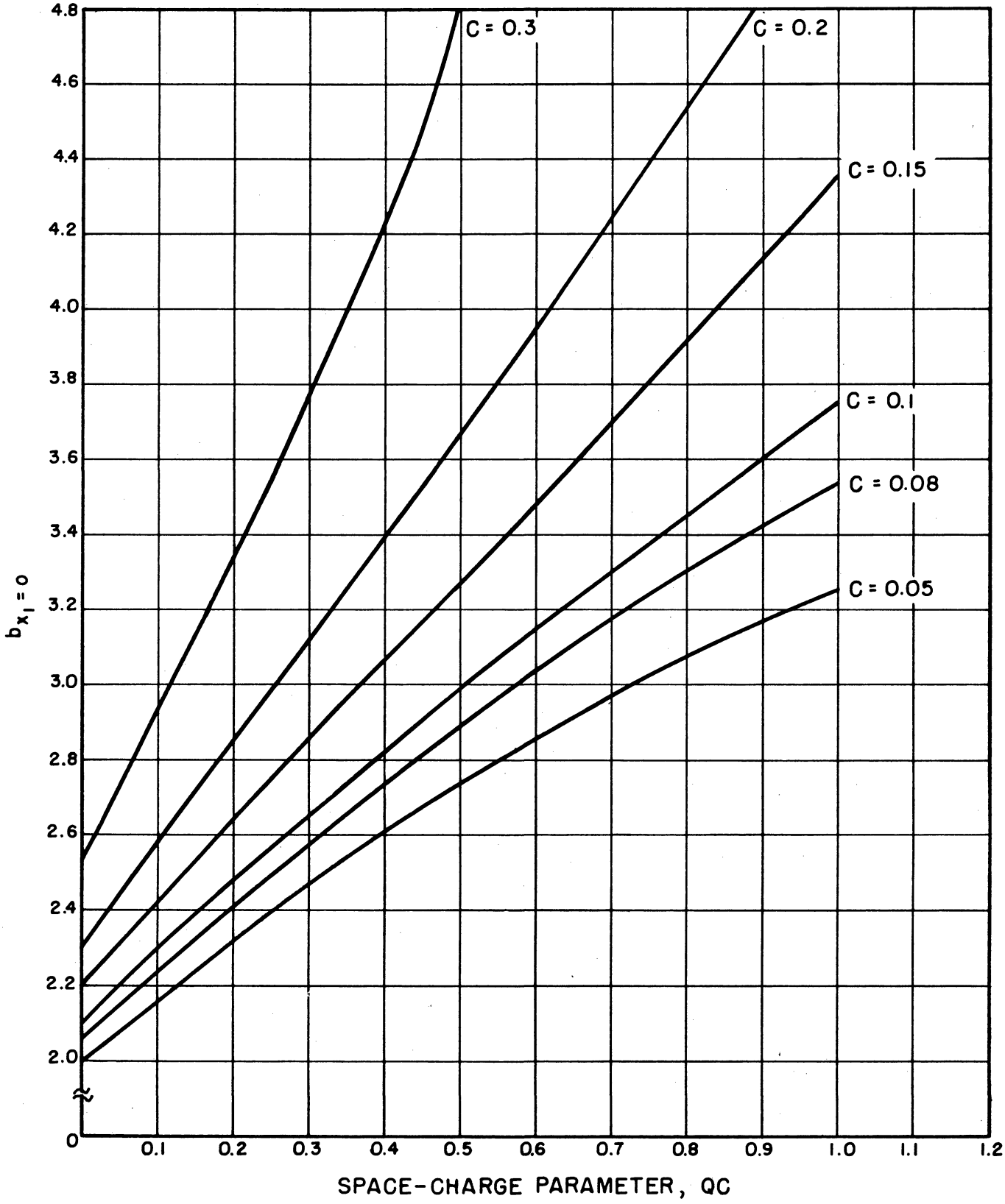

FIG. 8 $b_{x_1=0}$ VS. QC WITH C AS THE PARAMETER. (d = 0)

Maximum-gain curves for various values of C, QC, and d are shown in Figs. 9, 10, and 11. The gain decreases with increasing voltage and for very high voltage approaches zero asymptotically. As would be expected the gain increases with C and decreases as QC is increased. The effect of loss on the circuit is also seen to reduce the gain. The greatest gain occurs for a b slightly greater than that for which growing waves cease to exist. There is a smooth transition from the region of exponentially growing waves to the region in which the gain is a result of the beating of the three waves.

The effect of circuit loss on Crestatron gain is illustrated in Figs. 12 through 14 for a wide range of parameters. It is seen that the rate of decrease of gain is relatively independent of b, C and QC and is approximately 12 db per unit d. The loss in the absence of a stream is given by

$$\text{Loss in db} = \text{LN} = 54.6\ \text{CNd} \quad . \tag{27}$$

Since typical Crestatron lengths are in the vicinity of $\text{CN} \approx 0.4$ to 0.5 these data show that the signal decreases at the approximate rate of 24 db per unit d with no stream present. Hence the effect of circuit loss is to reduce the gain at only one-half the rate when the stream is present as compared with the rate of decrease of the signal in the absence of the stream. This compares favorably with the one-third figure for conventional traveling-wave tubes.

The gain for large positive values of b is a result of the combining of V_{c1}/V and V_{c2}/V, since V_{c3}/V is usually negligible. The magnitudes of these normalized voltages for a typical range of parameters are shown in Fig. 15. For large values of b it is seen from Fig. 15 that V_{c1}/V approaches zero and V_{c3}/V is still small, so that almost all the energy is in the second wave (circuit wave) V_{c2}/V. On the other hand for negative values of b (voltage below synchronism), the third wave (fast space-charge wave) V_{c3}/V predominates, as shown in Fig. 16.

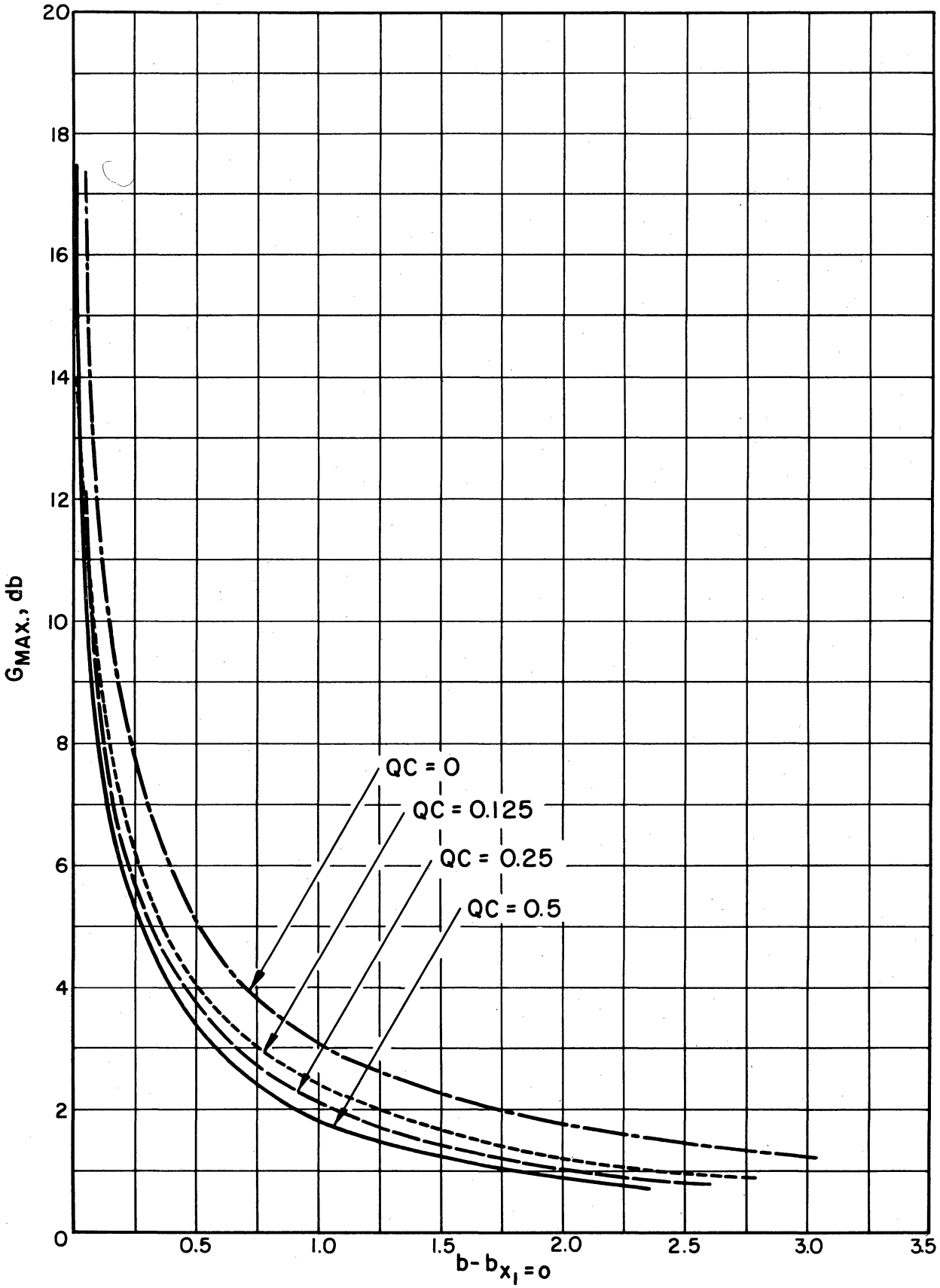

FIG. 9 MAXIMUM GAIN VS. $b - b_{x_1=0}$ WITH SPACE CHARGE AS THE PARAMETER. (C = 0.05, d = 0)

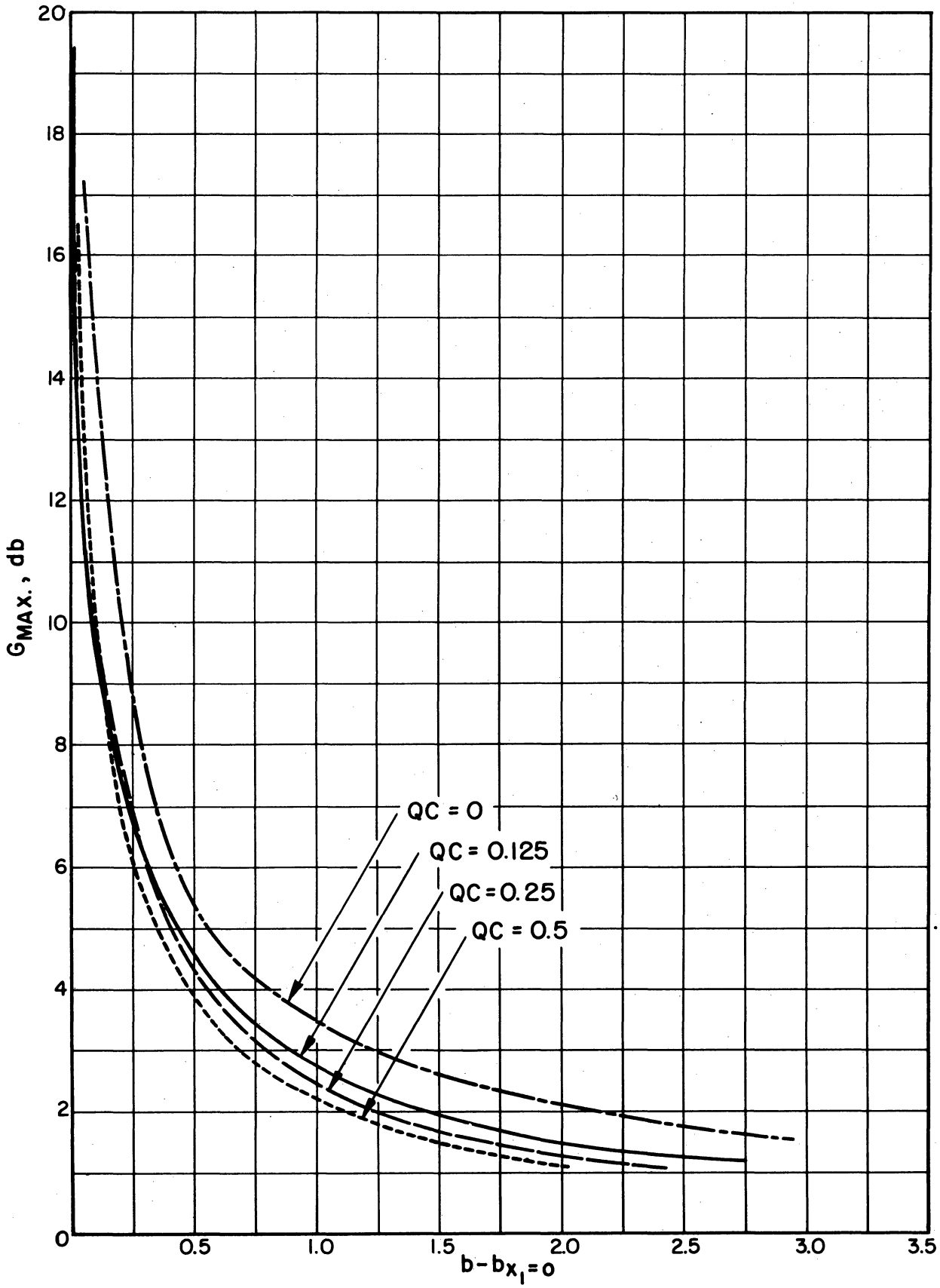

FIG. 10 MAXIMUM GAIN VS. $b - b_{x_1=0}$ WITH SPACE CHARGE AS THE PARAMETER. (C = 0.1, d = 0)

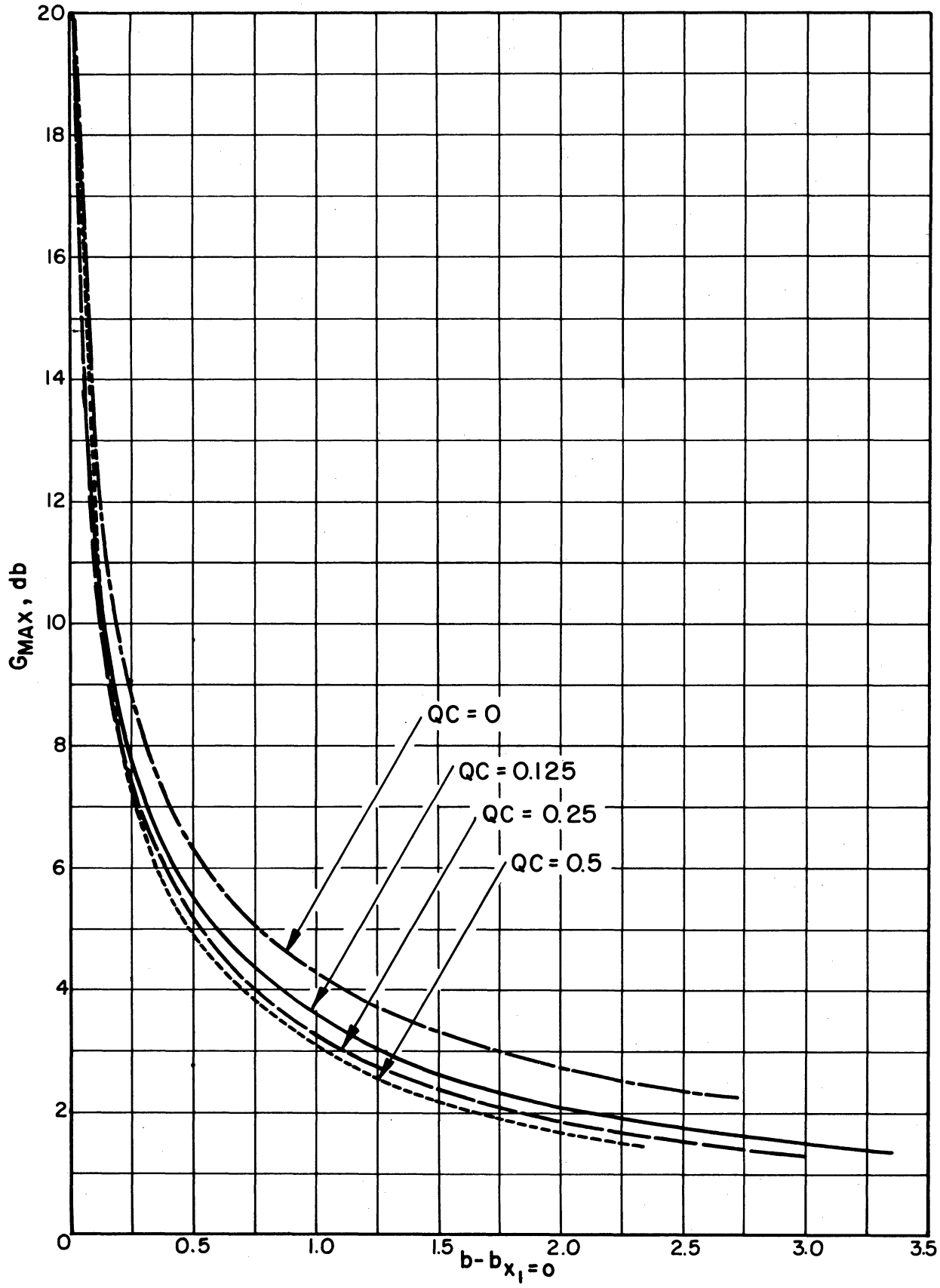

FIG. 11 MAXIMUM GAIN VS. $b - b_{x_1=0}$ WITH SPACE CHARGE AS THE PARAMETER. (C = 0.2, d = 0)

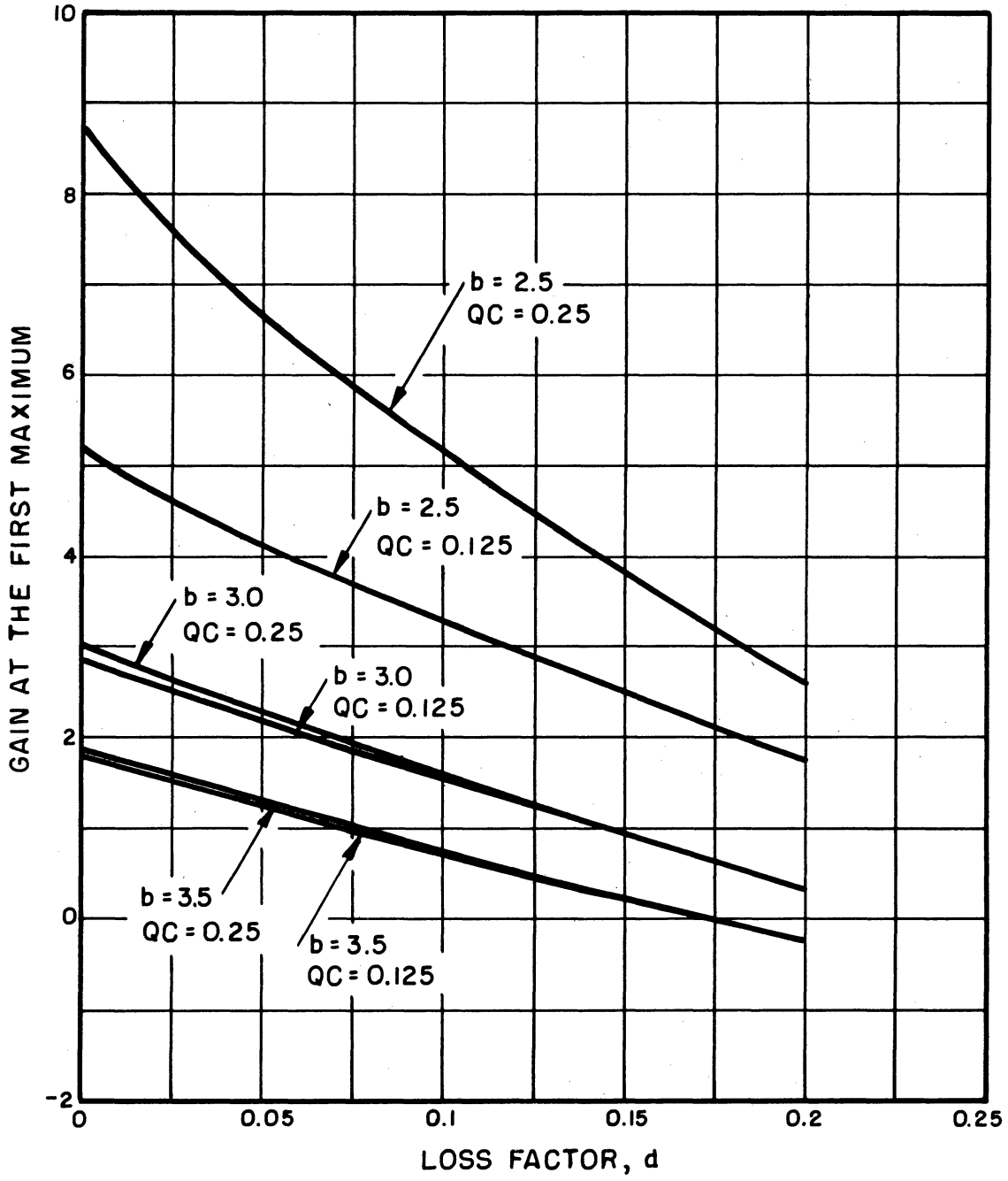

FIG. 12 EFFECT OF LOSS ON CRESTATRON GAIN. (C = 0.05)

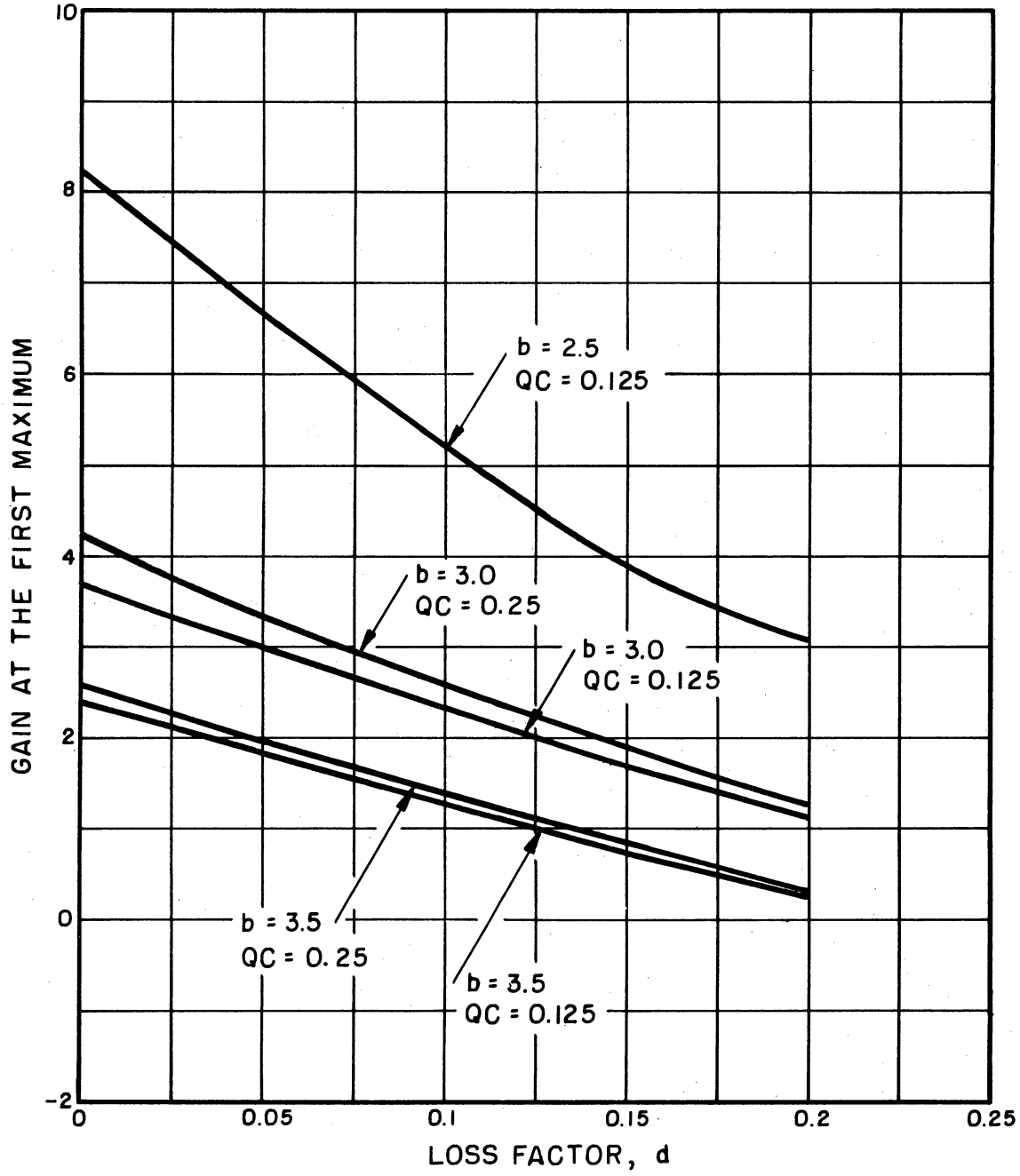

FIG. 13 EFFECT OF LOSS ON CRESTATRON GAIN. (C = 0.1)

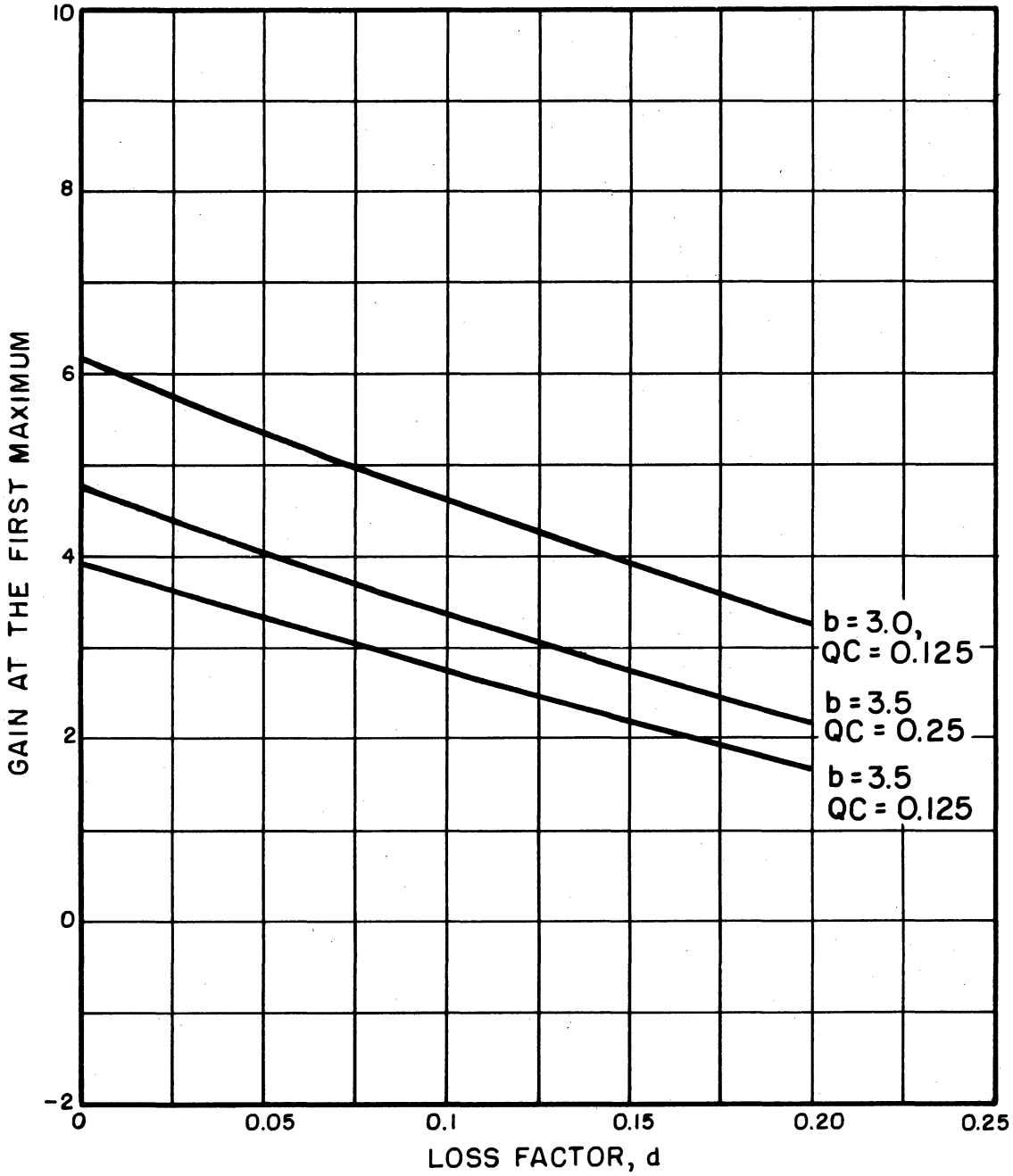

FIG. 14 EFFECT OF LOSS ON CRESTATRON GAIN. (C = 0.2)

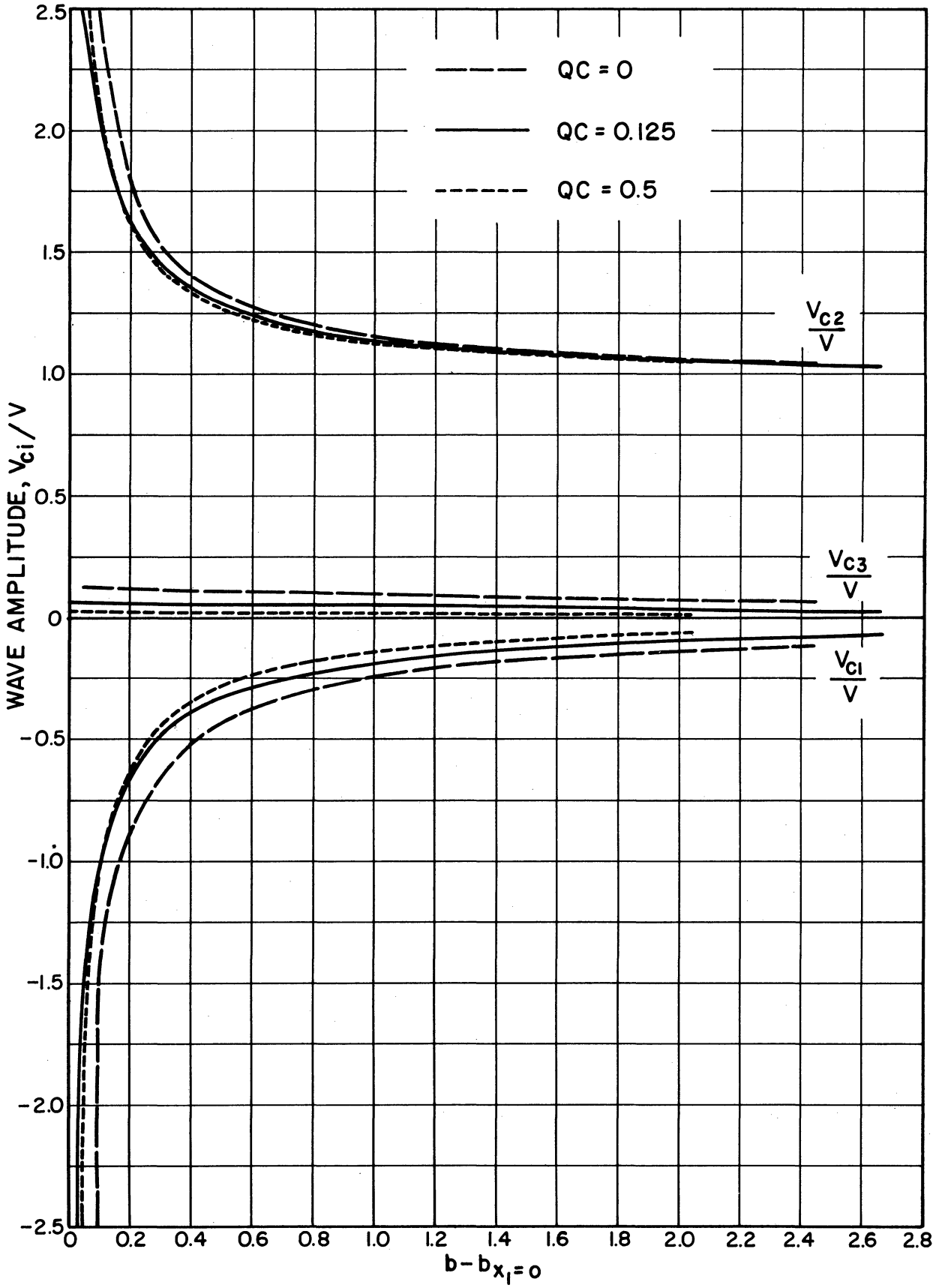

FIG. 15 NORMALIZED AMPLITUDES OF THE WAVE VOLTAGES VS. INJECTION VELOCITY. (C = 0.1, d = 0)

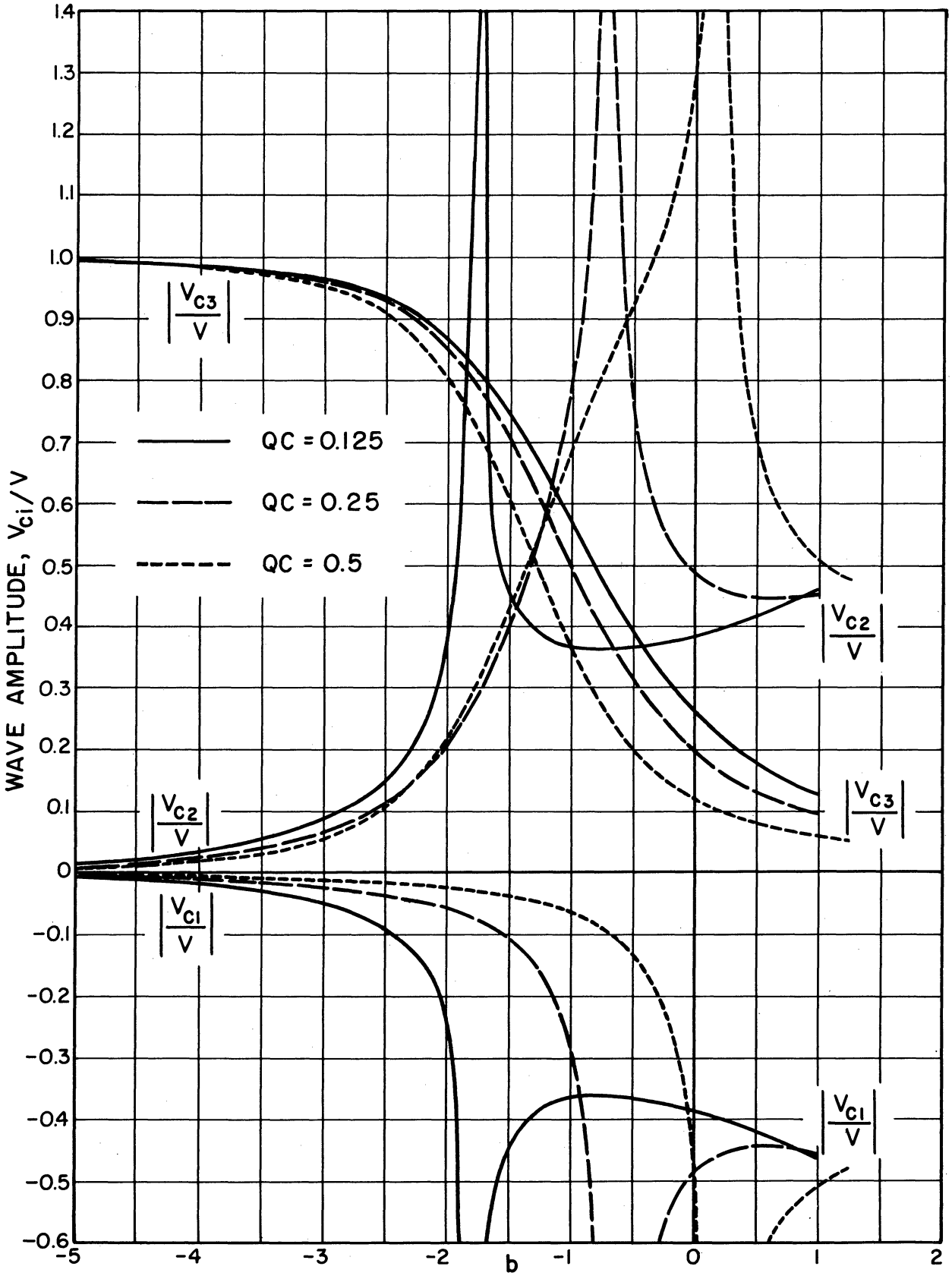

FIG. 16 NORMALIZED AMPLITUDES OF THE WAVE VOLTAGES VS. INJECTION VELOCITY. (C = 0.1, d = 0)

Typical plots of the distance to the first maximum of the gain curve are shown in Figs. 17, 18, and 19 for several values of C and space charge. The theoretical relation, Eq. 22, is also shown.

LARGE-SIGNAL PERFORMANCE

Saturation Gain. The large-signal performance of the Crestatron has been evaluated using the large-signal theory of the traveling-wave amplifier.[1] Significant large-signal gain is found for large values of $b > b_{x_1=0}$ when the input-signal level, ψ, is appreciable compared to CI_oV_o. A typical gain curve is shown in Fig. 20 with the input-signal level to the r-f structure as the parameter. A periodicity in the large-signal gain vs. distance curves is found similar to that previously shown with the linear theory. The gain is seen to decrease as the drive level is increased, but the power output and efficiency increase as the drive level is increased.

The composite results of the large-signal calculations may be plotted in summary form to show several interesting facets of the large-signal operation of the Crestatron. As seen in Figs. 21 and 22, the saturation gain as a function of the drive level to the r-f structure goes through a maximum at a value of ψ dependent upon the value of b. When the tube is operated at a "b" value which gives maximum small-signal gain or maximum saturation efficiency, an increase in the drive level results in a smooth transition to the Crestatron type of operation and the gain decreases smoothly.

It is useful also to plot the saturation gain vs. the velocity parameter with the drive level as the parameter. These results are shown in Figs. 23 and 24. For very high drive levels the gain is low and relatively independent of the injection velocity. This relationship is also in line with that predicted from the linear theory. The value of CN to the first maximum of the gain curve can also be plotted as a function of both the drive level and the

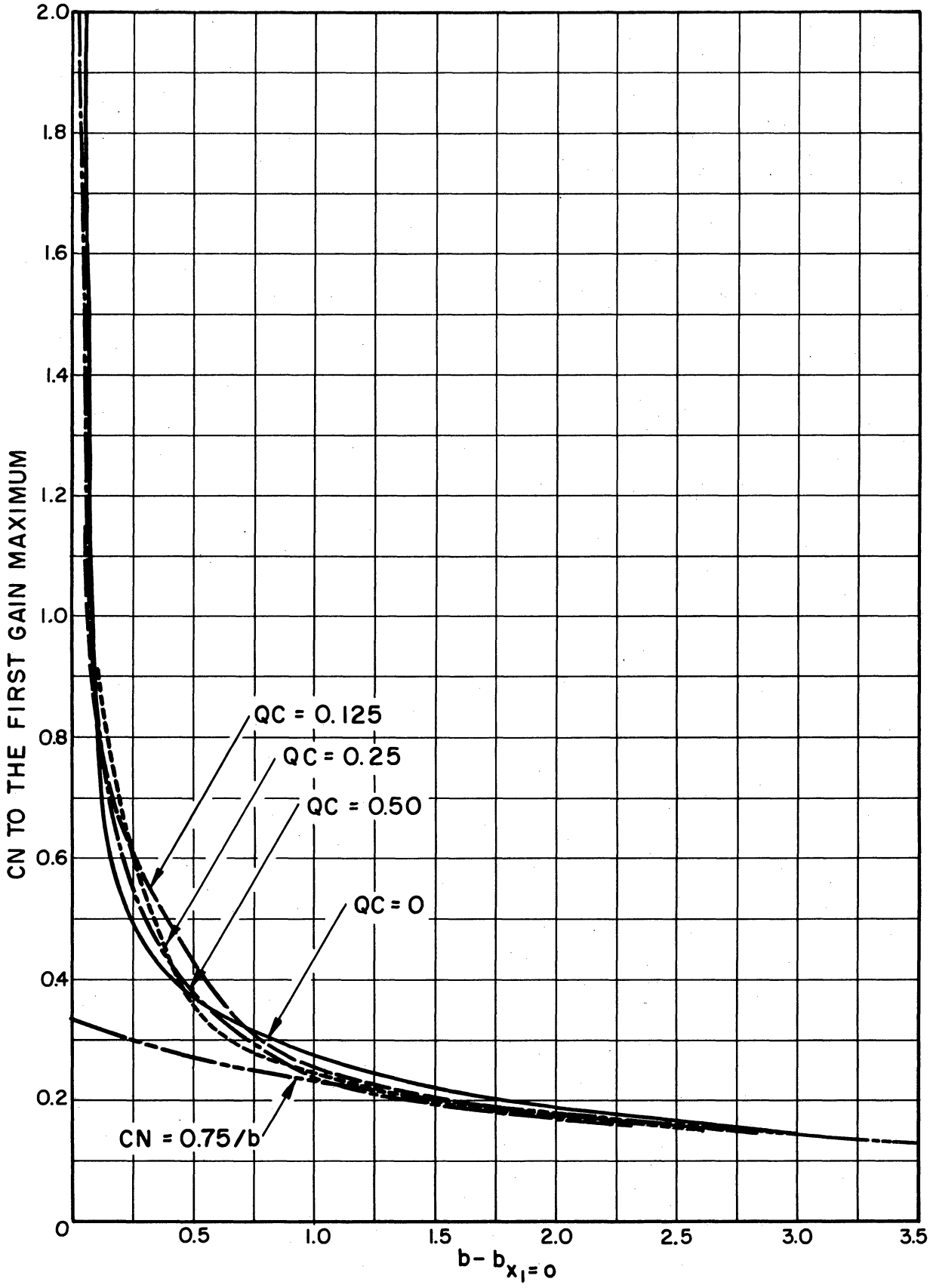

FIG. 17 CN TO THE FIRST GAIN MAXIMUM VS. INJECTION VELOCITY. (C = 0.05, d = 0)

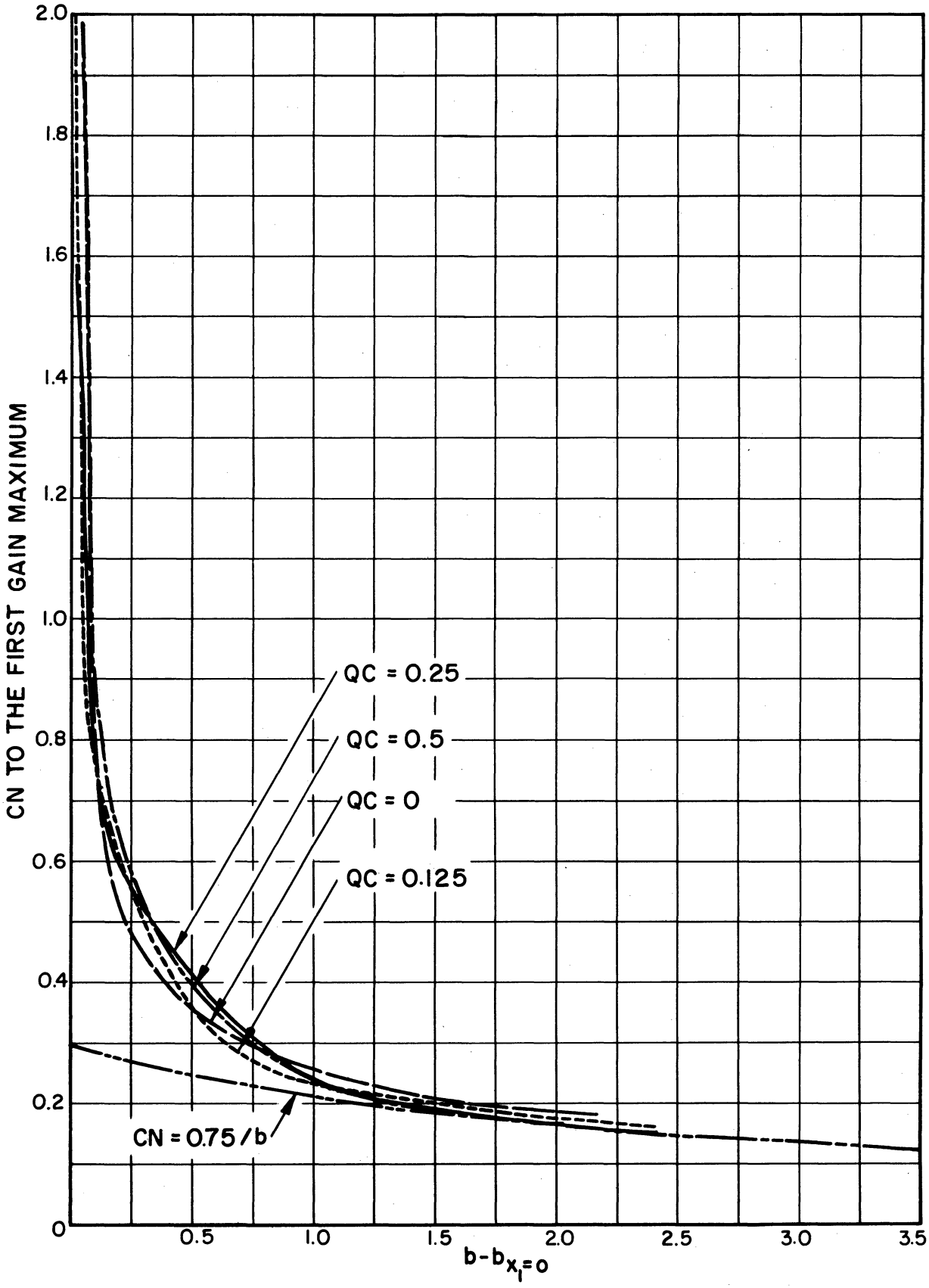

FIG. 18 CN TO THE FIRST GAIN MAXIMUM VS. INJECTION VELOCITY. (C = 0.1, d = 0)

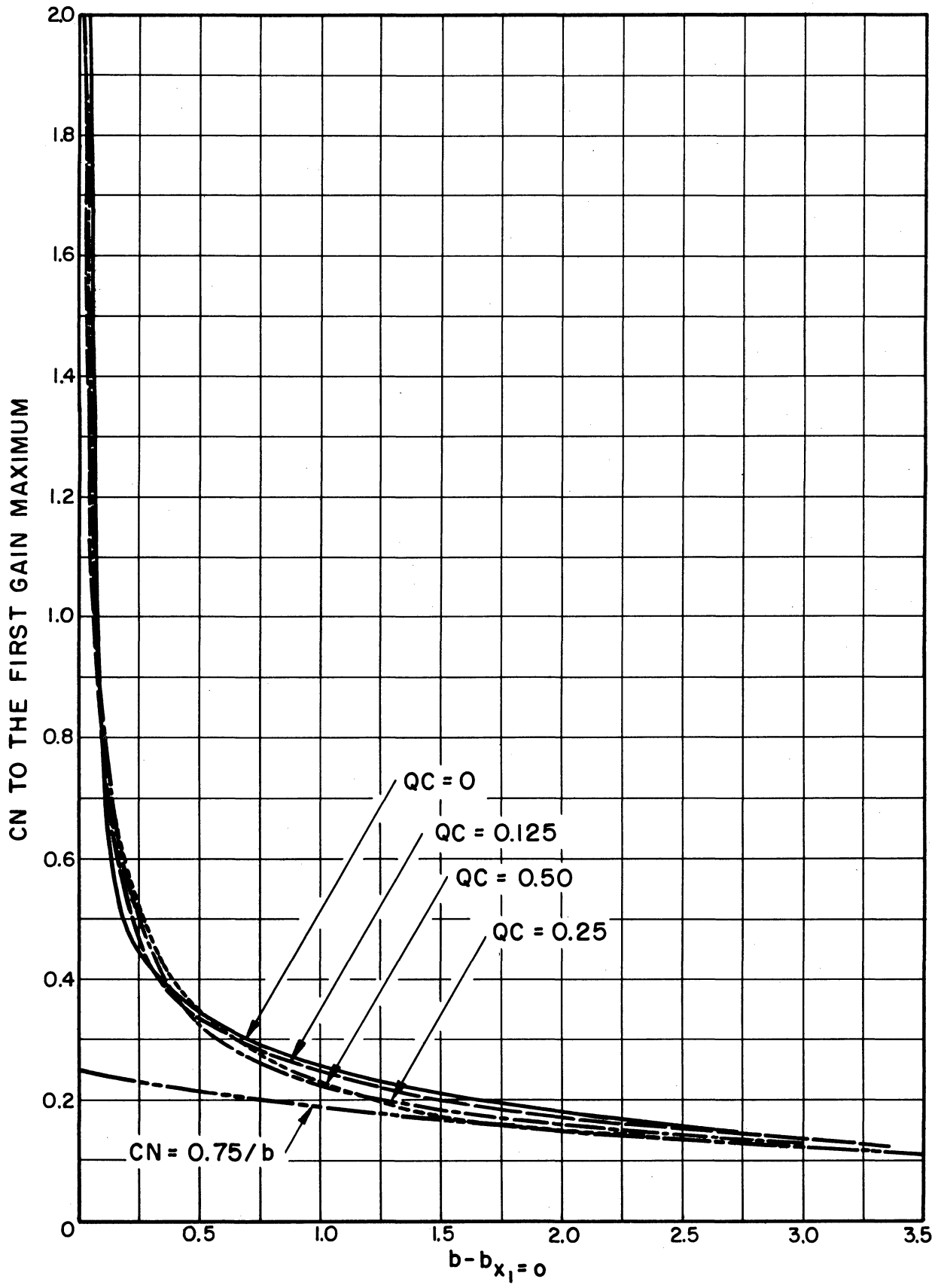

FIG. 19 CN TO THE FIRST GAIN MAXIMUM VS. INJECTION VELOCITY. (C = 0.2, d = 0)

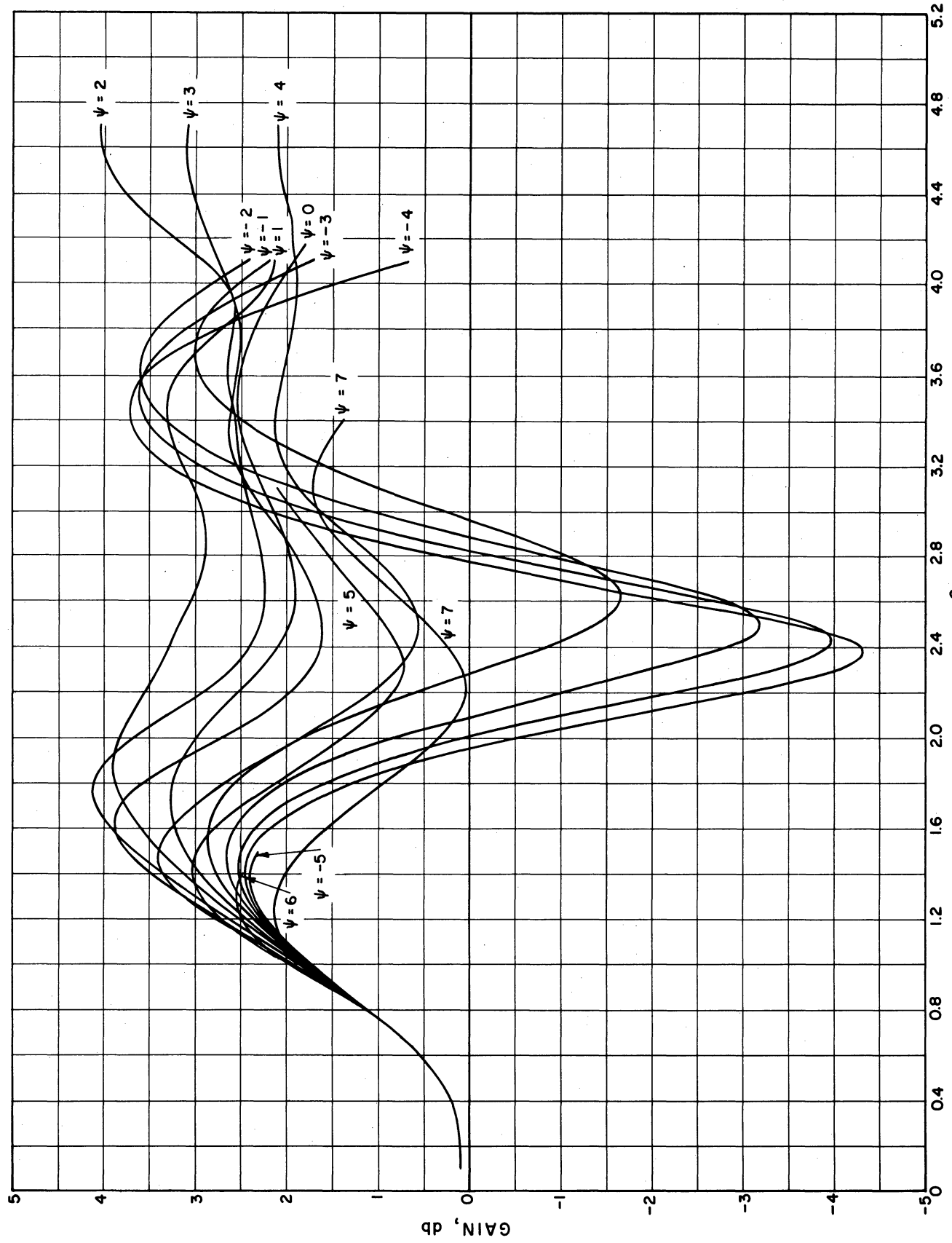

FIG. 20 LARGE-SIGNAL GAIN VS. LENGTH. (C = 0.1, QC = 0.25, B = 1.0, d = 0, b = 3.5)

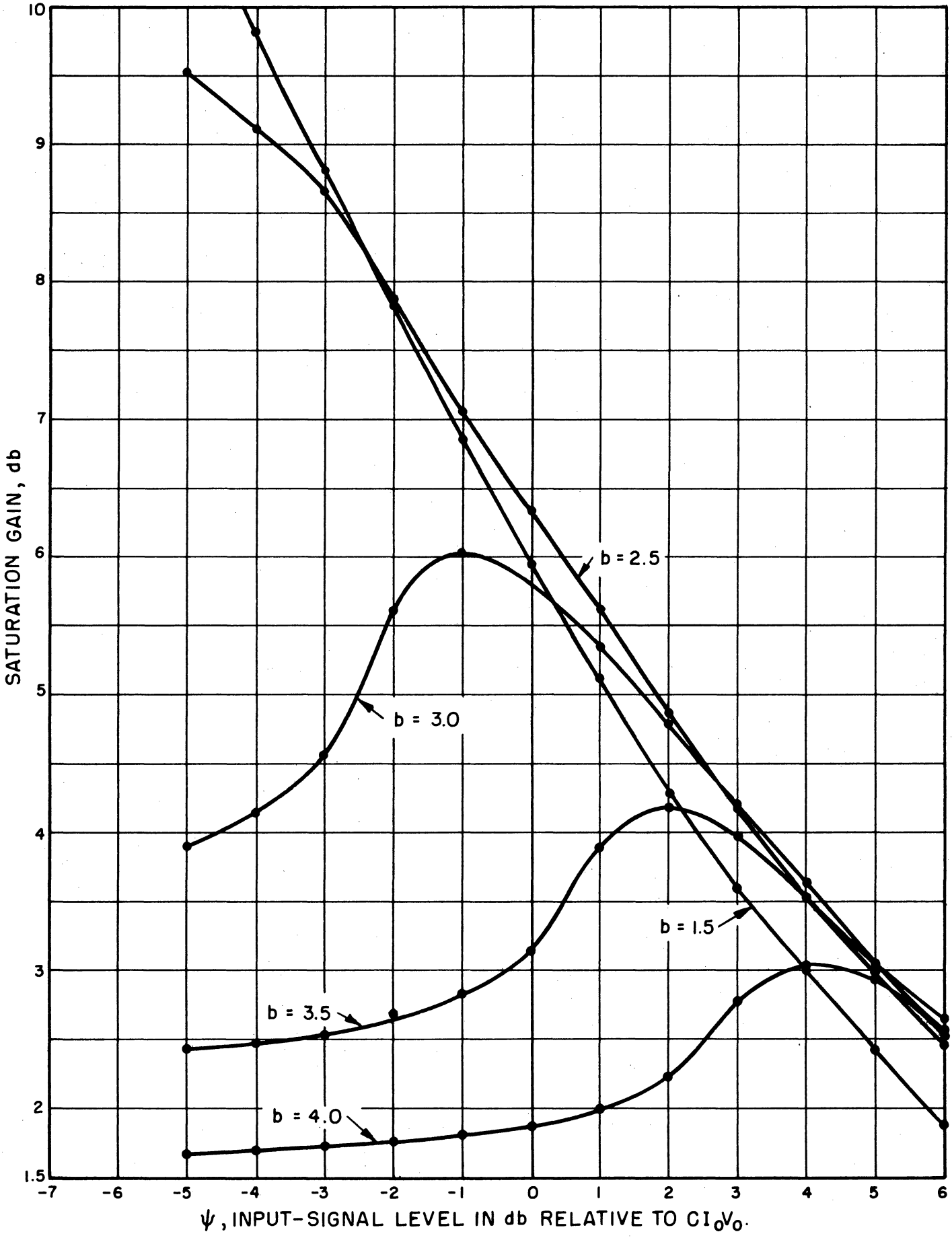

FIG. 21 SATURATION GAIN VS. INPUT-SIGNAL LEVEL WITH INJECTION VELOCITY AS THE PARAMETER. (C = 0.1, QC = 0.125, B = 1.0, d = 0, $b_{x_1=0} = 2.33$)

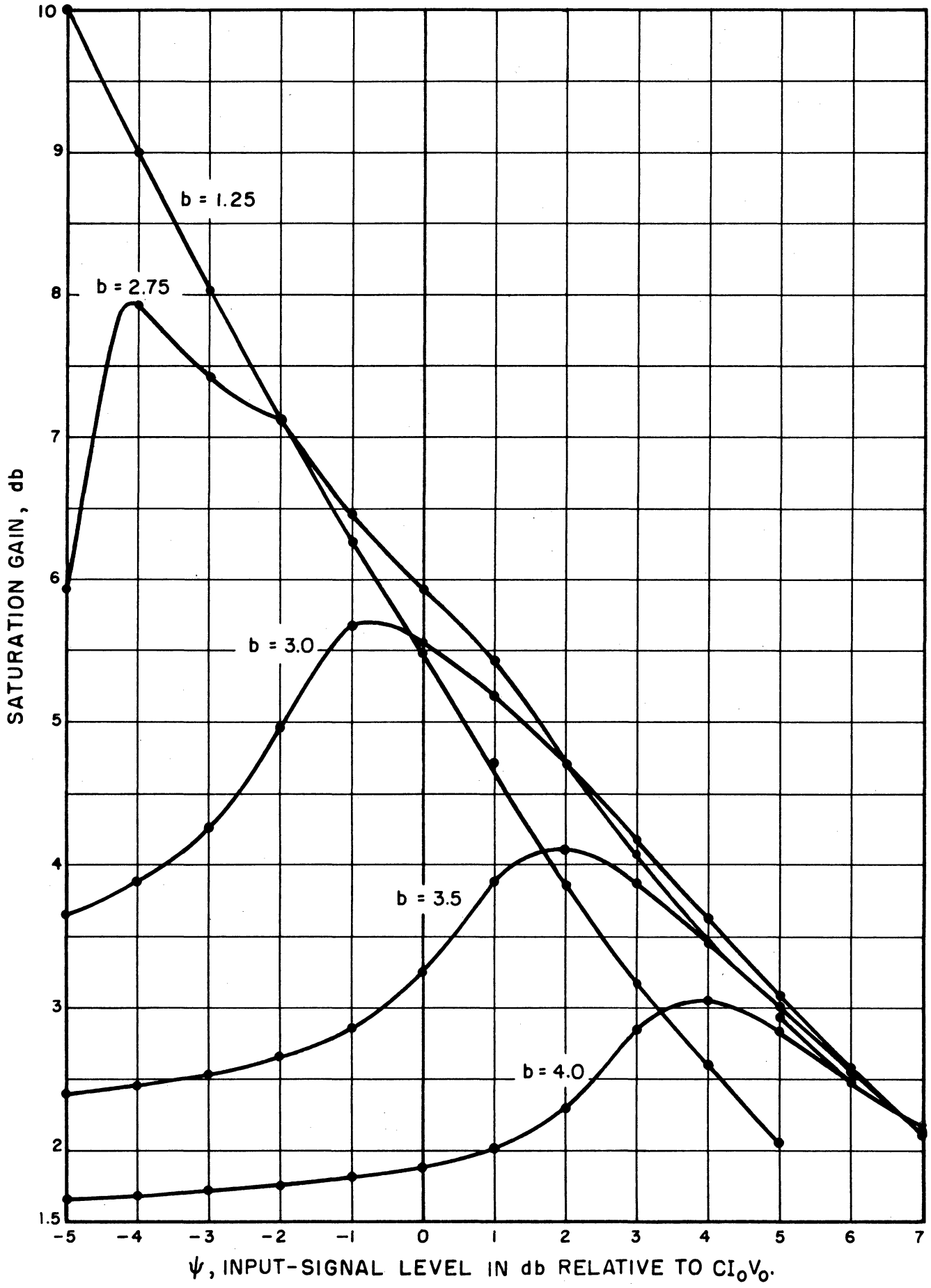

FIG. 22 SATURATION GAIN VS. INPUT-SIGNAL LEVEL WITH INJECTION VELOCITY AS THE PARAMETER. (C = 0.1, QC = 0.25, B = 1.0, d = 0, $b_{x_1=0}$ = 2.57)

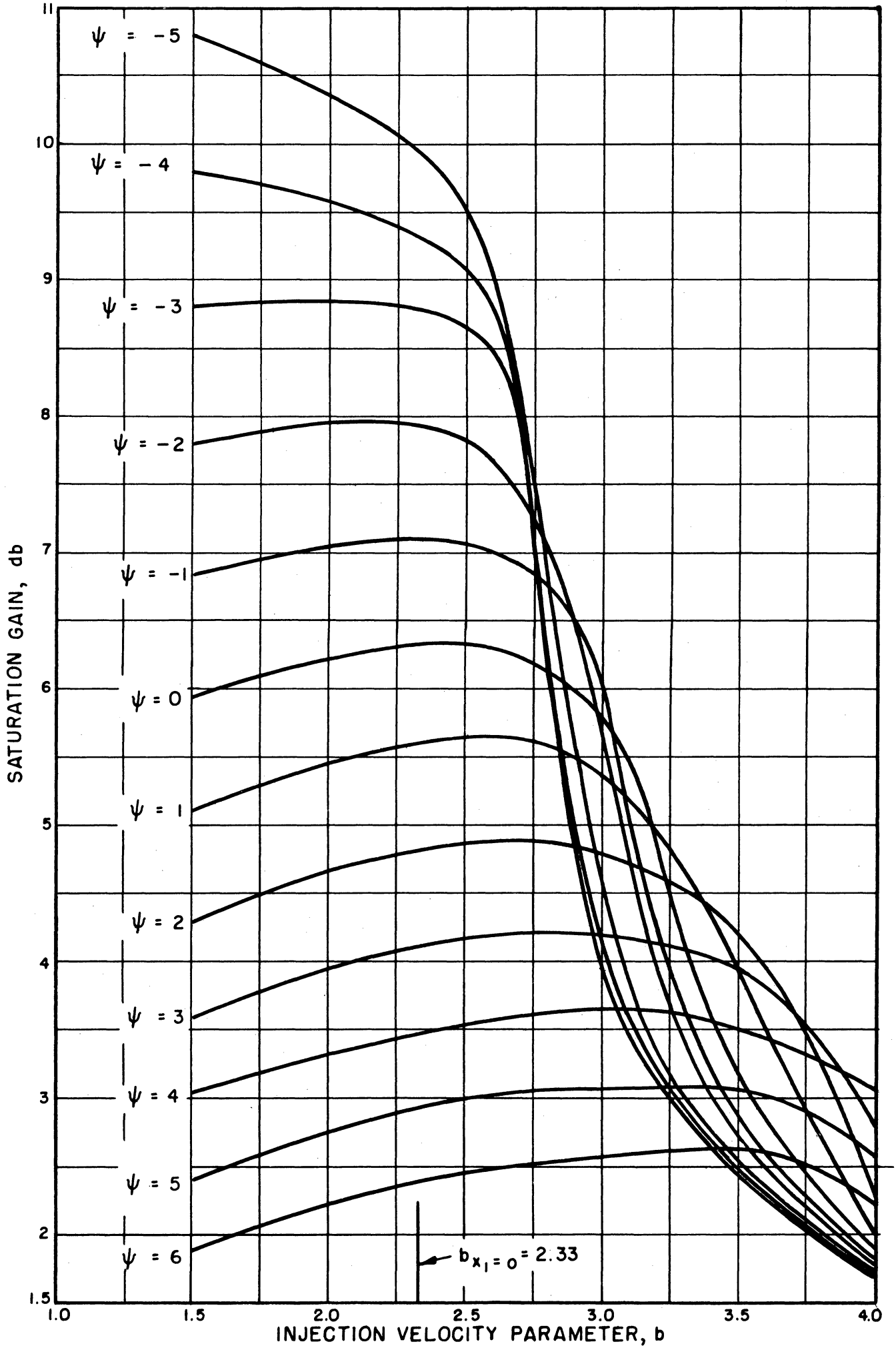

FIG. 23 SATURATION GAIN VS. INJECTION VELOCITY WITH INPUT-SIGNAL LEVEL AS THE PARAMETER. ($C = 0.1$, $QC = 0.125$, $B = 1.0$, $d = 0$, $b_{x_1=0} = 2.33$)

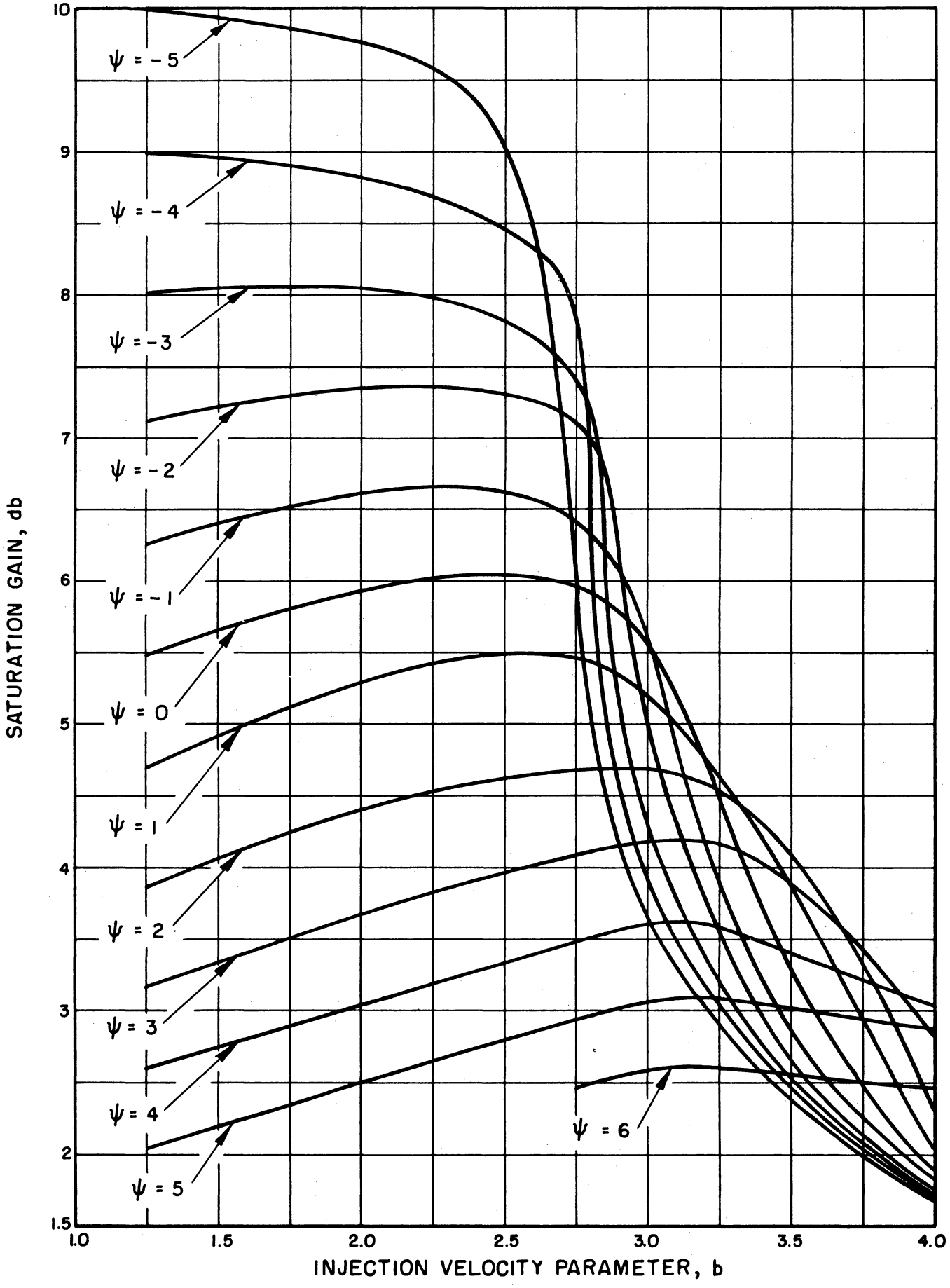

FIG. 24 SATURATION GAIN VS. INJECTION VELOCITY WITH INPUT-SIGNAL LEVEL AS THE PARAMETER. (C = 0.1, QC = 0.25, B = 1.0, d = 0, $b_{x_1 = o} = 2.57$)

value of b. These optimum-length curves are shown in Figs. 25 and 26.

A considerable amount of previously unexplained experimental information has been obtained by Caldwell and Hoch[2] which verifies the existence of gain in a forward-wave amplifier due to the beating between the waves propagating on the r-f structure. A comparison of the calculated gains using the linear and nonlinear theories along with some data extracted from Caldwell and Hoch's paper is presented in Fig. 27. It is seen that the agreement is very good between the theoretical results and the experimental data. Since the value of "d" was approximately 0.025 for the experimental data it is difficult to choose a reference b where x_1 is nearly zero. A value of b = 2.9 was used but had a larger value been used the agreement would have been even better.

Caldwell and Hoch found in addition that the saturation power output increased as the drive level was increased, keeping the voltage constant. This phenomenon is also predictable from the nonlinear theory; a comparison is shown in Fig. 28. The amount of increase in the saturation power level for input-signal levels comparable to and greater than CI_oV_o is some 4 db over that for very small input-signal levels. This increase in power output is probably due to the fact that this type of operation extracts the energy associated with all three circuit waves rather than only that of the growing wave as in the case of the conventional traveling-wave amplifier.

Efficiency. The saturation efficiency also increases as the drive level is increased, resulting in a relatively high efficiency for the Crestatron. Efficiency curves as a function of the drive level for constant values of the injection velocity are shown in Figs. 29 and 30. It is seen that the saturation efficiency for high drive approaches a value relatively independent of the value of b in the Crestatron. In calculating the saturation efficiency of the Crestatron the input power is significant and hence one must consider only the energy conversion

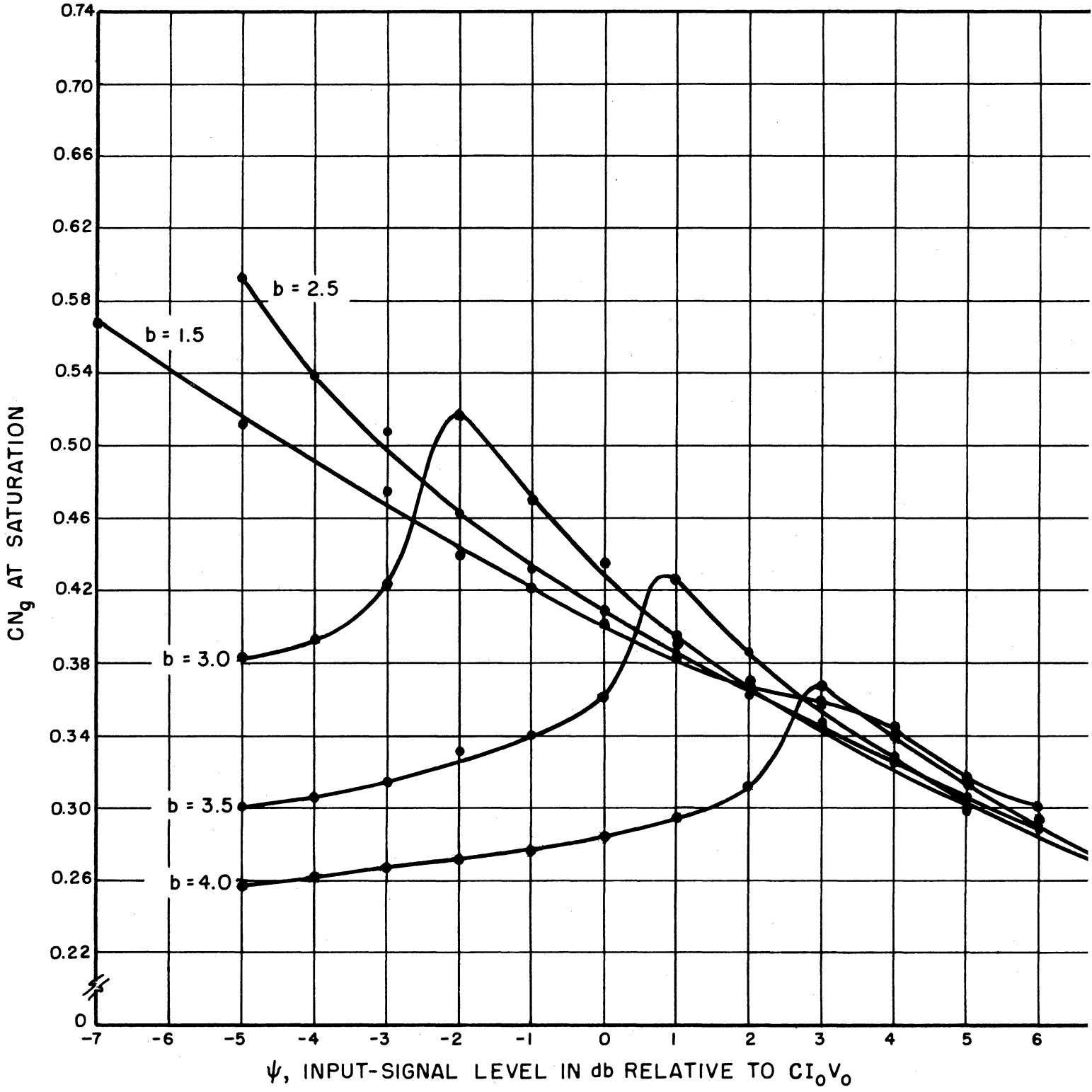

FIG. 25 SATURATION LENGTH VS. INPUT-SIGNAL LEVEL WITH INJECTION VELOCITY AS THE PARAMETER. (C = 0.1, QC = 0.125, B = 1.0, d = 0, $b_{x_1=0} = 2.33$)

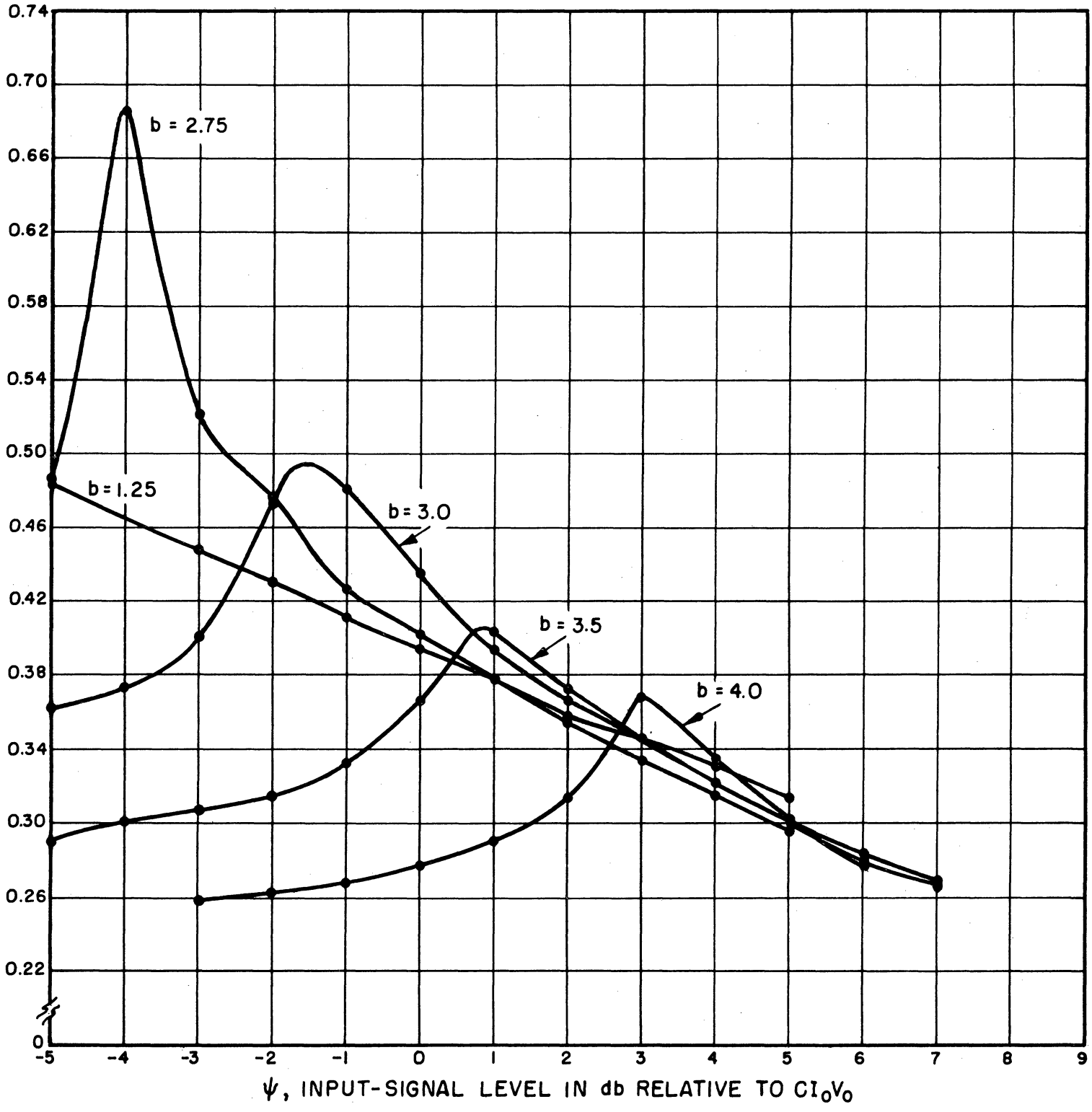

FIG. 26 SATURATION LENGTH VS. INPUT-SIGNAL LEVEL WITH INJECTION VELOCITY AS THE PARAMETER. (C = 0.1, QC = 0.25, B = 1.0, d = 0, $b_{x_1=0} = 2.57$)

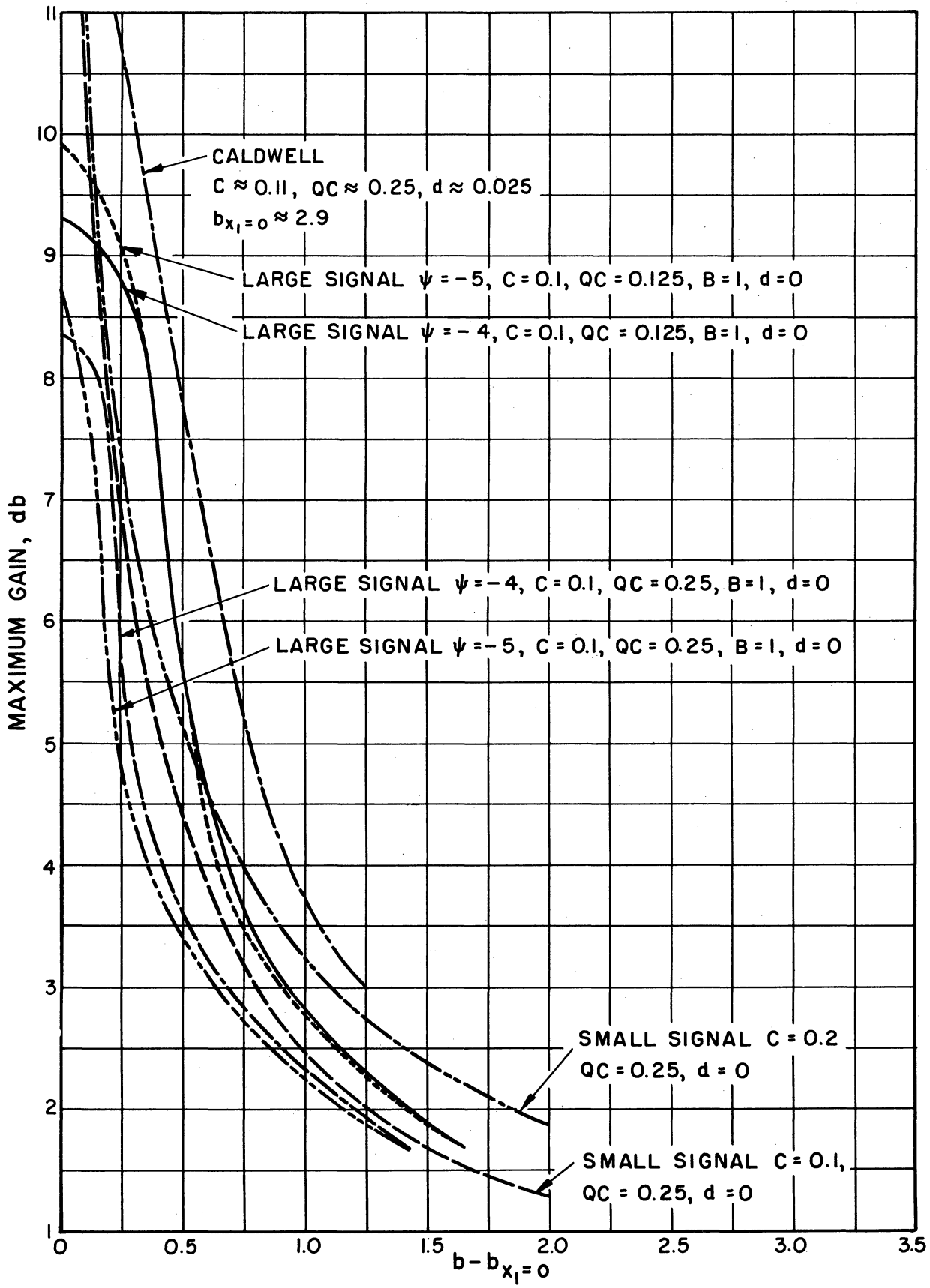

FIG. 27 COMPARISON OF THEORETICAL AND EXPERIMENTAL GAIN.

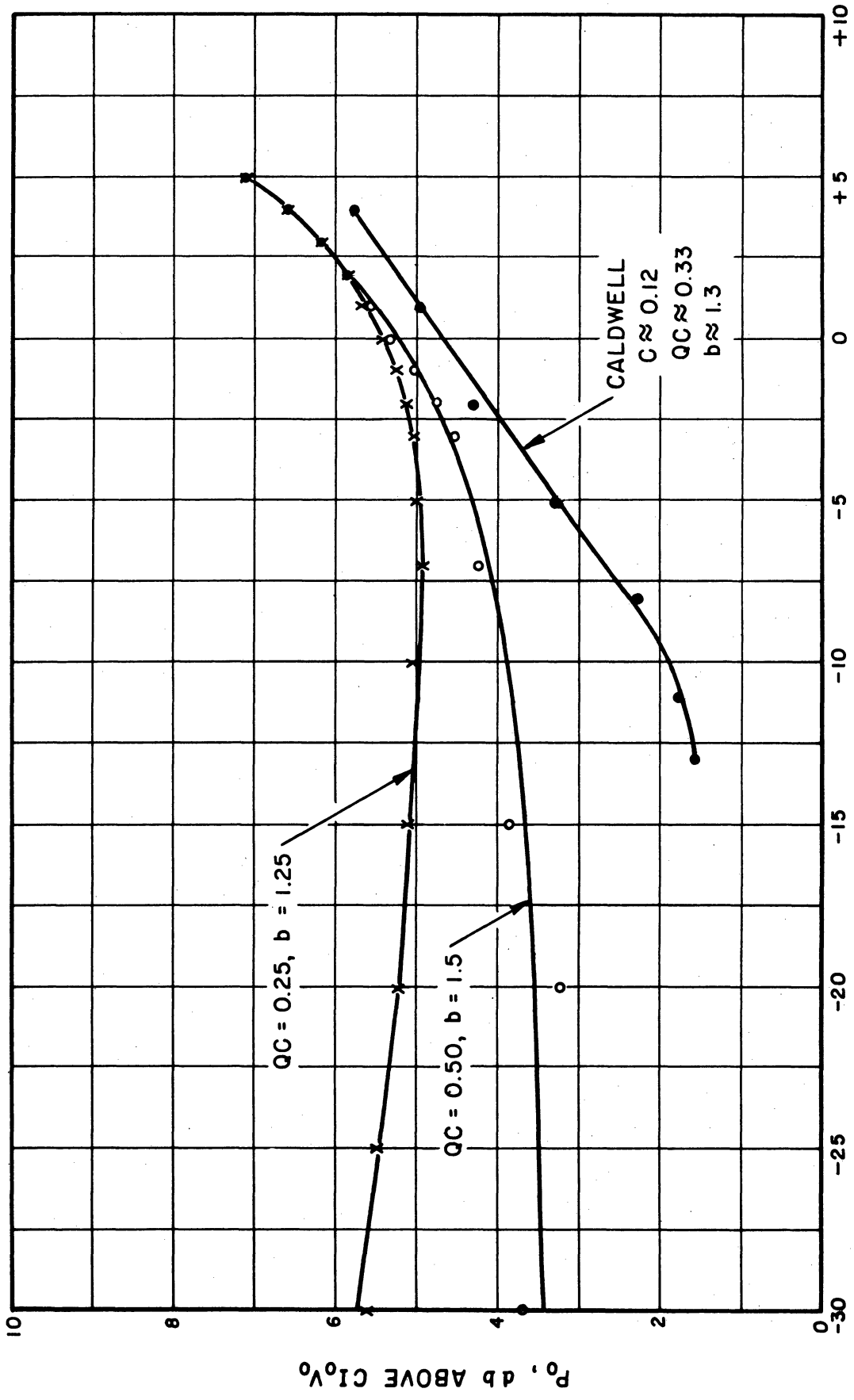

FIG. 28 VARIATION OF SATURATION LEVEL WITH INPUT-SIGNAL LEVEL.
(C = 0.1, B = 1.0, d = 0)

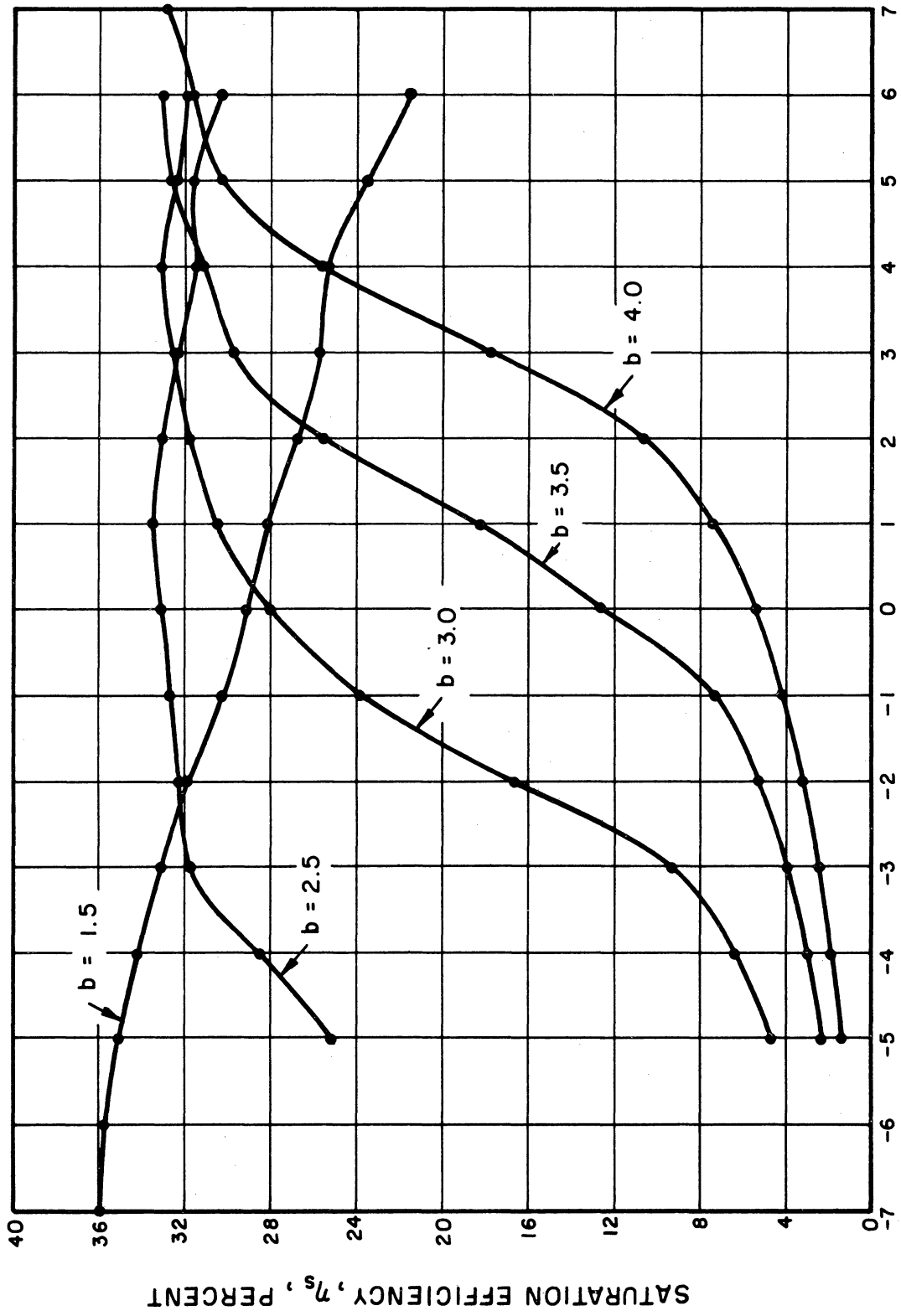

FIG. 29 SATURATION EFFICIENCY VS. INPUT-SIGNAL LEVEL WITH INJECTION VELOCITY AS THE PARAMETER. (C = 0.1, QC = 0.125, B = 1.0, d = 0, $b_{x_1=o} = 2.33$)

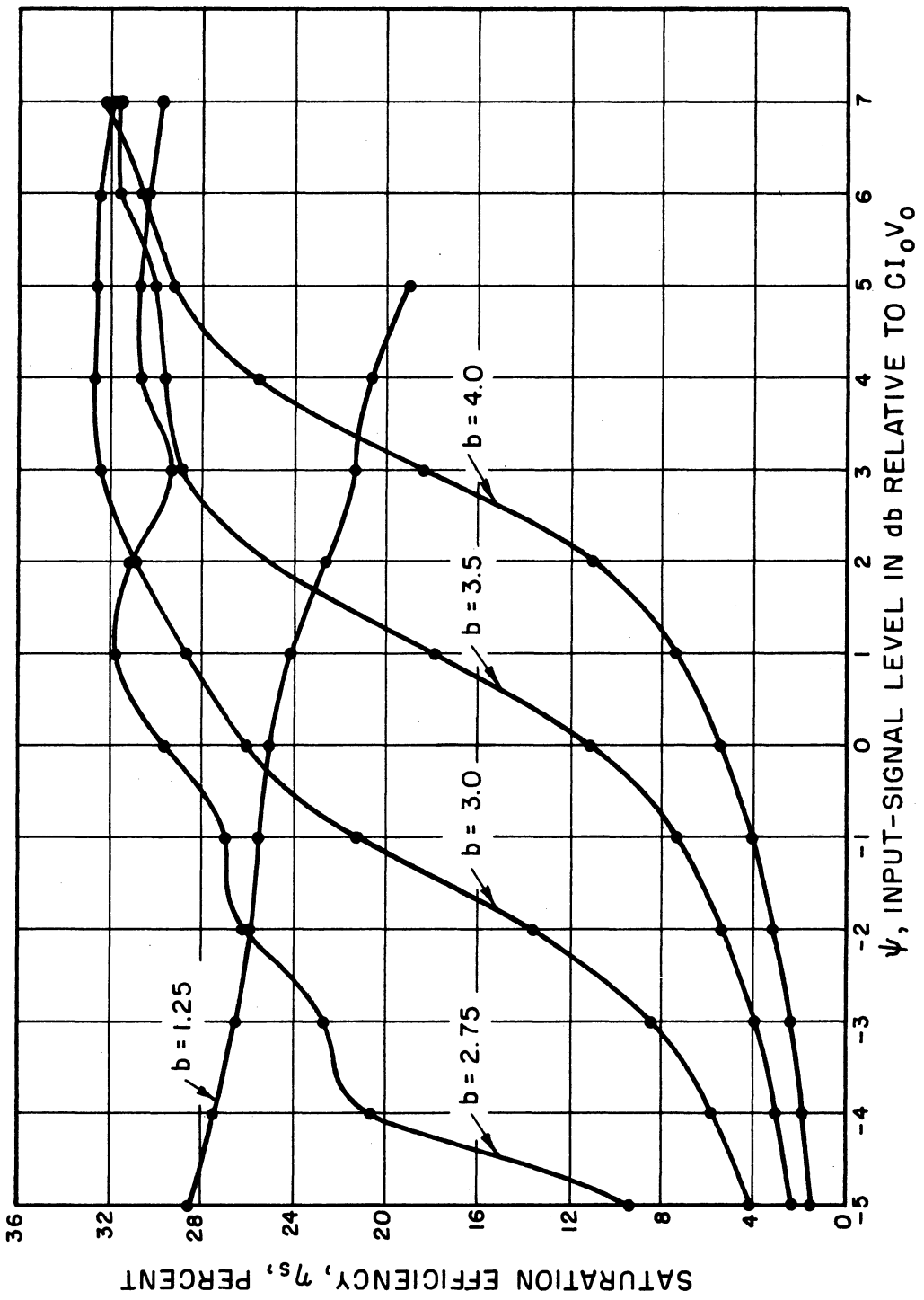

FIG. 30 SATURATION EFFICIENCY VS. INPUT-SIGNAL LEVEL WITH INJECTION VELOCITY AS THE PARAMETER. (C = 0.1, QC = 0.25, B = 1.0, d = 0, $b_{x_1=o} = 2.57$)

efficiency and subtract out the input-power level from the calculations. For values of b just slightly greater than that for which the wave growth constants become zero the efficiency is fairly constant as the drive level is varied. Continual increase in the drive power when b is adjusted for maximum saturation efficiency with small input-signal level results in a gradual decrease in the saturation efficiency. It is also interesting to plot the efficiency vs. b for particular values of drive as shown in Figs. 31 and 32.

The saturation efficiency is apparently higher at high values of drive when the voltage is adjusted for Crestatron-type operation than when the voltage is adjusted for maximum saturation output for a small input-signal level. This increase in efficiency is probably in part due to the fact that 1 + Cb is approximately 0.3 or 0.4 in the Crestatron, as opposed to around 0.2 in the growing wave mode of operation, and hence has considerably more energy to give up to the wave while slowing down.

CONCLUSIONS

A new type of forward-wave amplifier device has been developed and analyzed with both a linear and a nonlinear theory. The Crestatron operates on the basis of gain being produced by a beating between the three forward waves set up at the input of a traveling-wave amplifier operating at a high voltage so that there are no growing waves. The gains achievable are moderate and increase with increasing C but decrease with increasing QC. The gain also decreases as the injection velocity as measured by "b" is increased.

Nonlinear calculations indicate the same type of behavior as both the voltage and drive level are increased, and it has been shown that the saturation power output increased with the drive level. The saturation efficiency is high for this type of operation and the CN bandwidth can be as large as ± 50 percent.

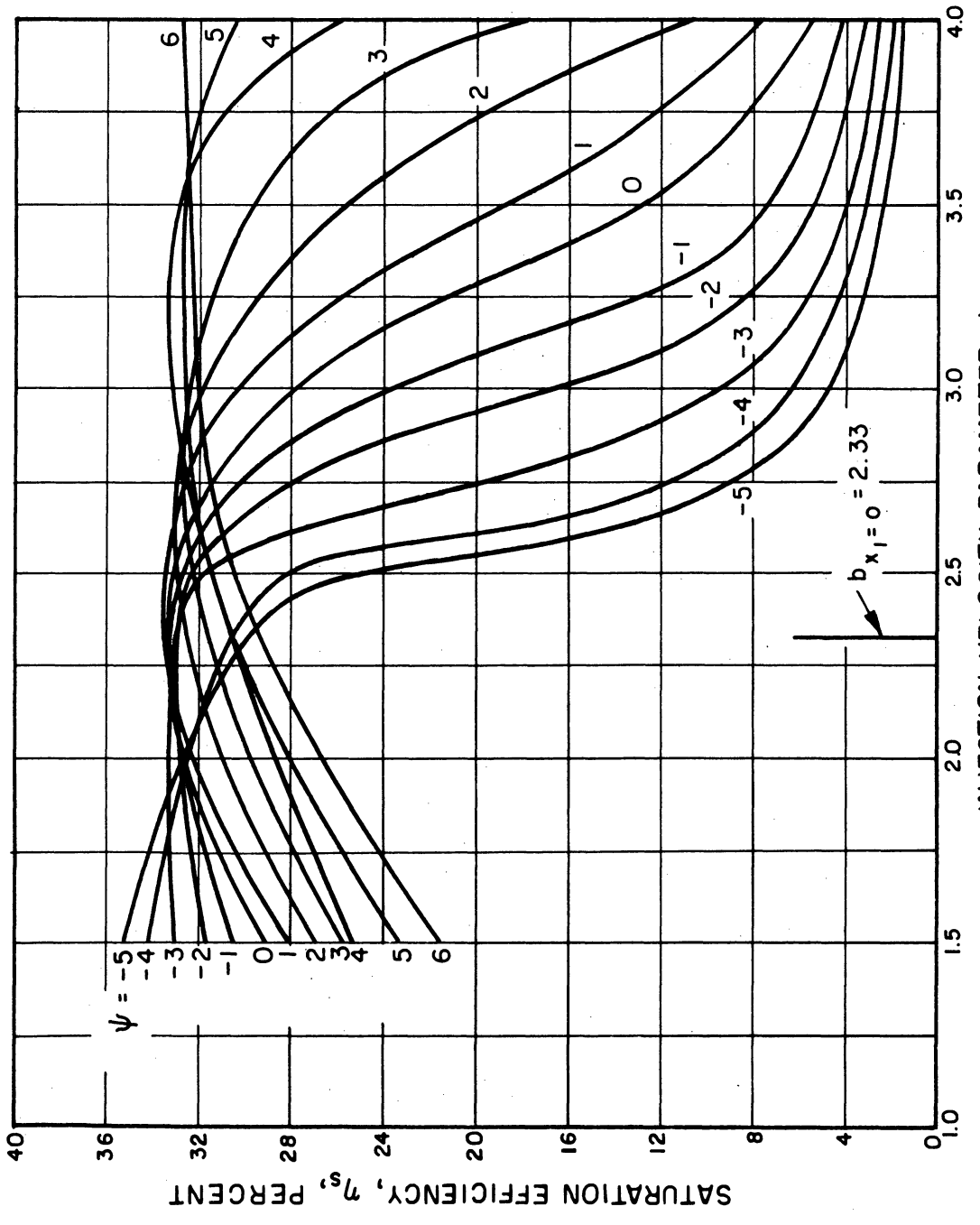

FIG. 31 SATURATION EFFICIENCY VS. INJECTION VELOCITY WITH INPUT-SIGNAL LEVEL AS THE PARAMETER. (C = 0.1, QC = 0.125, B = 1.0, d = 0, $b_{x_1=o} = 2.33$)

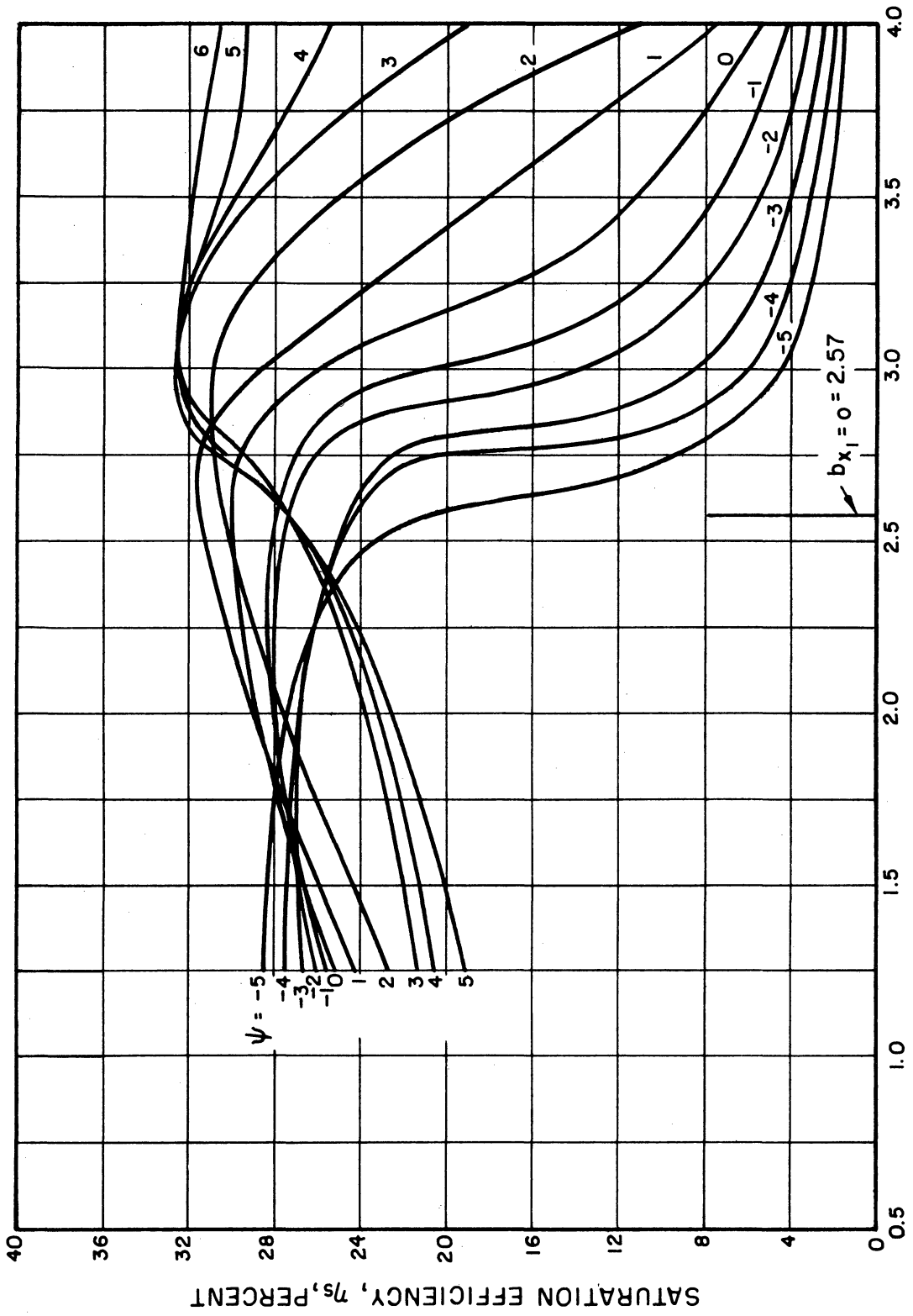

FIG. 32 SATURATION EFFICIENCY VS. INJECTION VELOCITY WITH INPUT-SIGNAL LEVEL AS THE PARAMETER. (C = 0.1, QC = 0.25, B = 1.0, d = 0, $b_{x_1=0}$=2.57)

The chief advantage of the Crestatron over the conventional traveling-wave amplifier is that its length is quite short for reasonable gains (4 to 6 wavelengths), which means that the focusing magnet can be of minimum length and weight and under certain conditions may even be eliminated.

ACKNOWLEDGMENTS

The author acknowledges the benefit of discussions, during the course of this work, with his associates in the Electron Tube Laboratory, and in particular the assistance of Messrs. Y. C. Lim and L. E. Stafford in solving the equations on a digital computer.

LIST OF SYMBOLS

$b = \frac{u_o - v_o}{C v_o}$	injection velocity parameter
C	gain parameter
d	loss parameter
F	helix impedance reduction factor
f	frequency
I_o	d-c stream current
$\tilde{i}$	r-f convection current in the beam
K_s	sheath-helix impedance
K_s'	normalized sheath-helix impedance
N	structure length in wavelengths
QC	space-charge parameter
u_o	stream velocity
V	input r-f voltage amplitude
V_{ci}	circuit component of wave amplitude
V_i	wave voltage amplitude
V_o	d-c stream voltage
$\tilde{v}$	r-f velocity in the beam
v_o	circuit characteristic wave phase velocity
z	distance measured from the input
$\beta = \omega/v$	wave phase constant
$\beta_e = \omega/u_o$	stream phase constant
Γ	wave propagation constant in the presence of the beam

LIST OF SYMBOLS

(Continued)

$\delta_i = x_i + jy_i$ wave incremental propagation constant

η charge-to-mass ratio of the electron

η_s saturation efficiency

$\Theta = 2\pi CN$ radian length of the tube

λ_g guide wavelength

λ_s stream wavelength

ω angular frequency

DISTRIBUTION LIST

No. Copies	Agency
3	Commander, Rome Air Development Center, ATTN: RCERRT, Griffiss Air Force Base, New York
1	Commander, Rome Air Development Center, ATTN: RCSSTW, Griffiss Air Force Base, New York
1	Commander, Rome Air Development Center, ATTN: RCSSLD, Griffiss Air Force Base, New York
8	Armed Services Technical Information Agency, Documents Service Center, Arlington Hall Station, Arlington 12, Virginia
1	Commander, Air Force Cambridge Research Center, ATTN: CRQSL-1, Laurence G. Hanscom Field, Bedford, Massachusetts
1	Director, Air University Library, ATTN: AUL-7736, Maxwell Air Force Base, Alabama
2	Commander, Wright Air Development Center, ATTN: WCOSI-3, Wright-Patterson Air Force Base, Ohio
2	Commander, Wright Air Development Center, ATTN: WCOSR, Wright-Patterson Air Force Base, Ohio
1	Air Force Field Representative, Naval Research Laboratory, ATTN: Code 1010, Washington 25, D. C.
1	Chief, Naval Research Laboratory, ATTN: Code 2021, Washington 25, D. C.
1	Chief, Bureau of Ships, ATTN: Code 312, Washington 25, D. C.
1	Commanding Officer, Signal Corps Engineering Laboratories, ATTN: Technical Reports Library, Fort Monmouth, New Jersey
1	Chief, Research and Development Office of the Chief Signal Officer, Washington 25, D. C.
1	Commander, Air Research and Development Command, ATTN: RDTDF, Andrews Air Force Base, Washington 25, D. C.
1	Commander, Air Research and Development Command, ATTN: RDTC, Andrews Air Force Base, Washington 25, D. C.
1	Director, Signal Corps Engineering Laboratories, ATTN: Thermionics Branch, Evans Signal Laboratory, Belmar, New Jersey
1	Secretariat, Advisory Group on Electron Tubes, 346 Broadway, New York 13, New York

DISTRIBUTION LIST
(Continued)

No. Copies	Agency
1	Chief, European, Air Research and Development Command, Shell Building, 60 Rue Cantersteen, Brussels, Belgium
1	California Institute of Technology, Department of Electrical Engineering, Pasadena, California, ATTN: Prof. L. M. Field
1	University of California, Electrical Engineering Department, Berkeley 4, California, ATTN: Prof. J. R. Whinnery
1	University of Colorado, Department of Electrical Engineering, Boulder, Colorado, ATTN: Prof. W. G. Worcester
1	Cornell University, Department of Electrical Engineering, Ithaca, New York, ATTN: C. Dalman
1	General Electric Company, Electron Tube Division of Research Laboratory, The Knolls, Schenectady, New York, ATTN: Dr. E. D. McArthur
1	General Electric Microwave Laboratory, 601 California Avenue, Palo Alto, California, ATTN: S. Weber
1	Huggins Laboratories, 711 Hamilton Avenue, Menlo Park, California, ATTN: L. A. Roberts
1	Hughes Aircraft Company, Electron Tube Laboratory, Culver City, California, ATTN: J. T. Milek
1	Varian Associates, 611 Hansen Way, Palo Alto, California, ATTN: Technical Library
1	Philips Research Laboratories, Irvington on the Hudson, New York, ATTN: Dr. Bernard Arfin
1	Columbia Radiation Laboratory, Columbia University, 538 West 120th Street, New York 27, New York, ATTN: Technical Library
1	University of Illinois, Department of Electrical Engineering, Electron Tube Section, Urbana, Illinois
1	University of Florida, Department of Electrical Engineering, Gainsville, Florida
1	Johns Hopkins University, Radiation Laboratory, Baltimore 2, Maryland, ATTN: Dr. D. D. King
1	Sperry Rand Corporation, Sperry Electron Tube Division, Gainsville, Florida

DISTRIBUTION LIST
(Continued)

No. Copies	Agency
1	Stanford University, Microwave Laboratory, Stanford, California, ATTN: Dr. M. Chodorow
1	Stanford University, Stanford Electronics Laboratories, Stanford, California, ATTN: D. A. Watkins
1	Raytheon Manufacturing Company, Tube Division, Waltham, Massachusetts, ATTN: Mr. Skoworon
1	Federal Telecommunications Laboratories, Inc., 500 Washington Avenue, Nutley, New Jersey, ATTN: T. Marchese
1	RCA Laboratories, Electronics Research Laboratory, Princeton, New Jersey, ATTN: Mr. E. H. Herold
1	Eitel-McCullough, Inc., San Bruno, California, ATTN: Mr. Donald Priest
1	Litton Industries, 960 Industrial Road, San Carlos, California, ATTN: Mr. Norman Moore
1	Massachusetts Institute of Technology, Research Laboratory of Electronics, Cambridge 39, Massachusetts, ATTN: Documents Library
1	Sperry Gyroscope Company, Great Neck, New York, ATTN: Engineering Library
1	Polytechnic Institute of Brooklyn, Microwave Research Institute, Brooklyn, New York, ATTN: Dr. G. Mourier
1	Harvard University, Cruft Laboratory, Cambridge, Massachusetts, ATTN: Technical Library
1	Sylvania Electric Products, Inc., Physics Laboratory, Bayside, New York, ATTN: Dr. Rudy Hutter
1	Sylvania Electric & Microwave Tube Laboratory, 500 Evelyn Avenue, Mountain View, California, ATTN: D. Goodman
1	Bell Telephone Laboratories, Inc., Murray Hill Laboratory, Murray Hill, New Jersey, ATTN: Dr. J. R. Pierce
1	University of Washington, Department of Electrical Engineering, Seattle, Washington, ATTN: A. E. Harrison
1	Massachusetts Institute of Technology, Lincoln Laboratories, Lexington 73, Massachusetts, ATTN: Mr. Robert Butman